From the Large Animal Clinic for Surgery

Faculty of Veterinary Medicine

University of Leipzig

MORPHOMETRIC ANALYSIS OF THE SHEEP THORACOLUMBAR SPINE USING COMPUTED TOMOGRAPHY AND A COMPARISON WITH THE HUMAN CORRELATE

Inaugural-Dissertation

to obtain the degree of a

Doctor medicinae veterinariae (Dr. med. vet)

from the Faculty of Veterinary Medicine
University of Leipzig

Submitted by

Mahmoud A. M. Abd El-Mageed
From Khartoum, Sudan

Leipzig, 2014

By approval of the Faculty of Veterinary Medicine, University of Leipzig

Dean: Prof. Dr. Manfred Coenen

Supervisor: Prof. Dr. Walter Brehm

Referees: Prof. Dr. Walter Brehm
Large Animal Clinic for Surgery
Faculty of Veterinary Medicine
University of Leipzig

Prof. Dr. Johanna Plendl
Institute for Veterinary Anatomy
Faculty of Veterinary Medicine
Free University of Berlin

Day of the defence: 08.07.2014

„ ... Mankind have not been given of knowledge except a little."

Quran 17:85

MY FAMILY

Contents

Abbreviations

3R principles	Replacement, Reduction, Refinement
CAM	Computed assisted myelography
CBT	Cortical bone thickness
CI	Concavity index
cm^3	Cubic centimetre
CSF	Cerebrospinal fluid
CT	Computed tomography
CV	Coefficient of variation
DT	Disc thickness
EI	Endplate index
Fig.	Figure
IV	Intravenous
Kg	Kilogram
kV	Kilovoltage
L	Lumbar vertebrae
mAs	Milliampere second
mg	Milligram
ml	Millilitre
mm	Millimetre
No.	Number
PAA	Pedicle axis angle
PAL	Pedicle axis length
PDH	Pedicle height
PDI	Pedicle index
PDL	Pedicle length
PDSD	Pedicle–dural sac distance
PDW	Pedicle width
ROM	Range of motion
SAC	Available space for dural sac
SCD	Spinal canal depth
SCI	Spinal canal index
SCW	Spinal canal width
T	Thoracic vertebrae
TPA	Transverse pedicle angle
TPL	Transverse process length
TVV	Tierversuchsvorhaben (Planned animal experiments)
VBD	Vertebral body depth
VBHd	Vertebral body height dorsal
VBHv	Vertebral body height ventral
VBW	Vertebral body width

1 Introduction

The development of specific implants and related implantation techniques for treatment of injured or diseased thoracolumbar spine has made enormous progress during recent years based on the experience acquired by the increase in the number of spinal surgeries (SÖYÜNCÜ et al., 2005). The clinical success of such operative procedures relies on the ability of spinal implants to achieve primary biomechanical stability in the affected levels (WILKE et al., 1998). New developed implants should therefore be tested before being brought into clinical practice to prove that they fulfil the main qualitative requirements such as long lasting local stability and biocompatibility as well as mimic the natural biomechanics. In this case, human spinal specimens would represent an ideal model for ex vivo testing of such implants as, the actual anatomy, size and kinematics, for which they are intended, are preserved. However, human specimens are difficult to obtain, especially from healthy younger population. Moreover the biological variability due to differences in age, sex, bone quality and disc and bone degenerative alterations limit the reliability of such experiments (SHENG et al., 2010). Therefore, homogeneous human specimens should be used or the number of specimens should be dramatically increased to overcome the aforementioned variability (ASHMAN et al., 1989). For these reasons, animal models have been introduced as a practical alternative, as higher homogeneity and availability are provided compared to human specimens. Standardization is effectively achieved by careful selection of breed, sex, age and weight (EGGLI et al., 1992; GURWITZ et al., 1993; EDMONDSTON et al., 1994). In addition, in vivo animal model experiments allow to evaluate the spinal implants in various biomechanical conditions for long period of time as well as to assess implant materials' biocompatibility, which cannot be tested in cadaveric specimens (PEARCE et al., 2007).

Various animal species have been used as animal models for human spinal research. Non-human primates, sheep, dogs, rats, mice, rabbits and pigs were used most frequently (KONRAD et al., 1987; GURR et al., 1988; WALL et al., 1998; MARTINI et al., 2001; REID et al., 2002; ROSSIGNOL et al., 2002; GANEY et al., 2003; BÖCKLER et al., 2007; SEEL et al., 2007; PERRETTA, 2009; NOUT et al., 2012; FRIGON, 2013; SOUBEYRAND et al., 2013). Animal model selection depends on many factors. SCHIMANDLEE and BODEN (1994) summarised them into availability, costs and care intensity of the animals, ethical matters, as well as ease of housing. For orthopaedic spinal research, particularly in implant testing, other factors play a significant role in animal model selection, such as the aim of the experiment, analogy to the human biological characteristics, size of the animal and its life span, which should suit the study duration.

MARTINI et al. (2001) reported the percentage of the animal models which were used in the period of 1970-2001 in the orthopaedic field. Noteworthy, the use of sheep is well established for assessment of new orthopaedic biomaterials and implants. In the period of 1990-2001, sheep were used in 9-12% of orthopaedic research in comparison with just over 5% in the 1980s.

Due to high morphological and biomechanical analogy as well as to similar body weight and size between humans and sheep (WILKE et al., 1997a; WILKE et al., 1997b; LEHMANN et al., 2008; MANUNTA et al., 2008), ovine spines have been most frequently used for in vivo and in vitro experiments (ASHMAN et al., 1989; EDMONDSTON et al., 1994; AHLGREN et al., 2000; AEBLI et al., 2006), especially for testing spinal implantology. The micro-architectural and biomechanical properties of the sheep spine were documented (WILKE et al., 1997a; MARTINI et al 2001), but only little is known about its morphometry. Therefore, a detailed knowledge of sheep spinal dimensions is essential for implant development and for standardising the use of sheep as model for spinal research.

2 Scientific Aspect of the study

2.1 Objectives

The current study aimed to provide:

- Quantitative morphometric data of the osseous structures of the sheep thoracolumbar spine.
- Volumetric analysis of the vertebral bodies of the sheep lumbar spine.
- A morphometric comparison of sheep lumbar spine with human published data in the literature.
- Morphometric dimensions of the sheep thoracolumbar dural sac.
- Anatomical relationship between the thoracolumbar dural sac and surrounding osseous structures of the spinal canal.

2.2 Hypothesis

Based on the biomechanics profile of the sheep thoracolumbar spine, the current study hypothesized that:

- The dimensions of the lumbar spine are larger than thoracic one.
- The lumbar vertebrae are safer for testing new spinal implants.
- The sheep lumbar vertebrae are comparable to human based on a morphometric point of view.

3 Publications

3.1 Publication 1: Morphometrical dimensions of the sheep thoracolumbar vertebrae as seen on digitised CT images

Mahmoud Mageed[1,2*], Dagmar Berner[1], Henriette Jülke[3], Christian Hohaus[4], Walter Brehm[1], Kerstin Gerlach[1]

Laboratory animal research 2013: 29(3), 138-147

http://dx.doi.org/10.5625/lar.2013.29.3.138

Pubmed ID: 24106508

[1]Large Animal Clinic for Surgery, Faculty of Veterinary Medicine, University of Leipzig, Leipzig, Germany.

[2]Department of Surgery and Anaesthesia, Faculty of Veterinary Medicine, University of Khartoum, Khartoum North, Sudan.

[3]Microsurgery and Animal Models Core, Translational Centre for Regenerative Medicine, University of Leipzig, Leipzig, Germany.

[4]Department of Neurosurgery, BG Hospital Bergmannstrost, Halle, Germany.

*Corresponding author: Mahmoud Mageed, Large Animal Clinic for Surgery, Faculty of Veterinary Medicine, University of Leipzig, An den Tierkliniken 21, D-04103, Leipzig, Germany. Tel: +49-341-9738264; Fax: +49-341-9738218; Email: mahmoud.mageed@hotmail.com

Received May 20, 2013

Revised June 13, 2013

Accepted July 05, 2013

Abstract

The sheep spine is widely used as a model for preclinical research in human medicine to test new spinal implants and surgical procedures. Therefore, precise morphometric data are needed. The present study aimed to provide computed tomographic (CT) morphometry of sheep thoracolumbar spine. Five adult normal Merino sheep were included in this study. Sheep were anaesthetised and positioned in sternal recumbency. Subsequently, transverse and sagittal images were obtained using a multi-detector-row helical CT scanner. Measurements of the vertebral bodies, pedicles, intervertebral disc and transverse processes were performed with dedicated software. Vertebral bodies and the spinal canal were wider than they were deep, most obviously in the lumbar vertebrae. The intervertebral discs were as much as 57.4% thicker in the lumbar than in the thoracic spine. The pedicles were higher and longer than they were wide over the entire thoracolumbar spine. In conclusion, the generated data can serve as a CT reference for the ovine thoracolumbar spine and may be helpful in using sheep spine as a model for human spinal research.

Keywords: Ovine, spine anatomy, animal model, reference values, computed tomography

In vitro experiments are useful in providing basic understanding of the biomechanical and functional features of the spine, and thus more insight into the physiological and pathological functions. Furthermore, new spinal implants and surgical procedures are often tested pre-clinically on cadaver spines [1,2].

Human specimens are preferable for these models because they mimic the physiological situation as much as possible. However, there are some difficulties in using the human model, such as obtaining it fresh especially from a healthy population and in large quantities in order to obviate the wide scattering effect associated with biological variability [3]. Moreover, *in vitro* studies do not provide time-dependent changes of biomechanics, histological and functional behaviour after applying instruments [4]. Therefore, animal models represent a suitable alternative, these being available and having more uniform geometrical and mechanical properties than humans when selected for breed, age and weight [5-8].

To mimic the human spine, an appropriate animal should be used which has biomechanical characteristics and anatomical dimensions of the spine as similar as possible to those in humans. Furthermore, precise geometrical data of animal models are needed for mathematical models [9,10]. The sheep spine is frequently used as a model for human spinal orthopaedic researches and is well accepted due to similarities with humans in weight, bone and joint structure and the bone remodelling process [11-14] Moreover, sheep are easily available, inexpensive, easy to handle and well accepted as an ethical animal model [15].

Computed tomography (CT) is a non-invasive imaging modality which has been used extensively in human to perform *in vivo* morphometric analysis of the spine [16,17] and describe the normal variation in size and shape of the human vertebrae at various spinal levels [18-20].

Measurement accuracy represents the core of morphometric studies. Therefore, the factors affecting the accuracy should be addressed. The accuracy of the measurements based on CT images is affected by scanning parameters [21] and viewer control setting [22].

Morphometry of sheep thoracolumbar spine is essential for the design and interpretation of results derived from studies which contemplate their use. This study aims to provide quantitative reference values of healthy ovine thoracolumbar using CT.

Materials and Methods

Animals and anaesthesia

To reduce the numbers of animals, 5 female Merino sheep without any history or clinical signs related to spinal diseases were included. The mean age of the sheep was 2.0±0.1

year. Mean body weight was 62.0±5.3 kg. The study was approved by the Animal Protection Agency regional office Leipzig.

Each sheep was fasted for 24 hours and deprived of water for 12 hours before being premedicated with 0.1 mg/kg atropine sulphate (Atropinum sulfuricum 0.5 mg Eifelango®, Eifelango, Bad Neuenahr-Ahrweiler, Germany), and a combination of 0.1 mg/kg butorphanol tartrate (Alvegesic®, CP-Pharma GmbH, Burgdorf, Germany) and 0.2 mg/kg midazolam (Midazolam, B. Braun; B. Braun, Melsung, Germany) administered intravenously. Anaesthesia was induced with 3 mg/kg ketamine chlorhydrate (Ursotamin®, Serumwerk Bernburg AG, Bernburg, Germany) intravenously. After endotracheal intubation, anaesthesia was maintained with isoflurane (Isofluran CP®, CP-Pharma GmbH) delivered in oxygen through an endotracheal tube.

CT examination

The sheep were positioned in sternal recumbency and intravenous fluid bags were used to obtain a perpendicular position of the spine relative to the x-ray beam of the gantry. Contiguous slices were obtained from the cranial aspect of T2 to the caudal aspect of L6 with a multi-detector-row helical CT unit (Philips Medical Systems MX8000 IDT 16, Hamburg, Germany). Technical settings were 120 kV, 200 mA, 0.75 second tube rotation and a pitch of 0.438. The data were reconstructed to a transverse and sagittal image series with slice thickness ranging between 0.3-1.2 mm using a high-frequency image reconstruction algorithm (bone). Window width and level settings were standardised for all measurements (window width, 2000 Hounsfield units; window level, 500 Hounsfield units). The CT images were reconstructed using multi planar reconstruction in transverse and sagittlal planes. Transverse images were reconstructed parallel to the cranial endplate of the vertebral body, whereas the sagittal images were reconstructed at two levels. The first level was at the midsagittal plane of the vertebra to measure some of the vertebral body and intervertebral disc dimensions. The second level was at the midsagittal plane of the left or right pedicle for measuring the pedicle height, whereby we assumed there was no difference between the left and right pedicle. Subsequently, CT images were transferred to a work station and reviewed with dedicated software (CuraSmartClient curasystems GmbH, Ettlingen, Germany). From the transverse images series, a single CT image through the mid level of the cranial third of the pedicle was selected for measuring. This level demonstrates individual features of each vertebra relative to adjacent vertebra.

Eleven parameters were measured from the transverse images and four parameters from the sagittal images for each spinal level (Table 1, Figure 1-5). Parameters of the vertebral body, spinal canal and transverse processes were measured as described in human literature [23].

The vertebral body measurements (Figure 1,2) included the distance between the lateral borders of the vertebral body in the transverse plane of the cranial endplate, termed the vertebral body width (VBW), and the distance between the dorsal and ventral borders of the vertebral body, termed the vertebral body depth (WBD). The distance between the cranial and caudal endplates of the vertebral body at the dorsal margin was measured from the sagittal image was termed the vertebral body height dorsal (VBHd). The same distance at the ventral margin was termed the vertebral body height ventral (VBHv). Cortical bone thickness (CBT) was assessed as the distance between the outer and inner borders of the lateral part of the vertebral body on the transverse image. Disc Thickness (DT) was measured at the middle level of the intervertebral disc on the sagittal image. In this study, DT refers to the disc which located cranial to the mentioned vertebral level. The spinal canal parameters included spinal canal width (SCW) and depth (SCD) and were measured on transverse images (Figure 3). SCW was measured as the distance between the axial pedicle cortices, while SCD was defined as the distance from the dorsal border of the vertebral body to the lamina at the midline. Transverse process length (TPL) was the distance between the tips of the transverse processes measured on the transverse image (Figure 3).

The pedicle width (PDW) was also measured on the transverse image of each vertebra as the narrowest part of the pedicle (Figure 4). The pedicle height (PDH) was measured on the sagittal image in the same manner as PDW. The pedicle axis length (PAL) was measured from the dorsal cortex of the articular facet to the midpoint of the ventral vertebral body cortex on the transverse plane, while the angle between PAL and the vertebra sagittal midline was defined as the pedicle axis angle (PAA) (Figure 4). According to the location of the pedicle to the transverse process, the vertebrae were divided into types I and II. In type I, the pedicles were located ventrally to the transverse process. The pedicle length (PDL) was therefore measured as a distance between the dorsal pedicle cortex and the perpendicular line to the vertebral midline, which is tangent to the ventral border of the spinal canal (Figure 5). In type II, the pedicles were located dorsally to the transverse process. Thus, the PDL was measured as a distance between the dorsal pedicle cortex and junction point of the ventral border of the transverse process and vertebral body (Figure 4). The angle between the line halvings the pedicle and vertebral sagittal midline in the transverse plane was termed transverse pedicle angle (TPA). Each parameter was measured six times by the same observer (MM).

Statistical analysis

Intra-observer reliability was calculated. For each sheep three vertebral levels per parameter were randomly selected to detect the intra-observer reliability which was represented by the

coefficient of variation (CV). One-way analysis of variance and the Scheffe test were used to determine differences between the vertebral levels for each parameter. Commercially available software was used for statistical analysis (Microsoft Excel 2010, Microsoft Deutschland GmbH, Unterschleissheim, Germany). The level of significance was set at $P<0.0001$.

Results

Repeated measurements of spinal parameters revealed a high level of reliability, where CV values of all parameters were less than 5% (Table 1). In Tables 2-4, mean and standard deviation of the CT measurements in thoracolumbar spines of the investigated 5 Merino sheep are presented.

The maximum value of VBHd was observed at L6 and the smallest at T3. VBHd was fairly constant at about 25 mm in the cranial thoracic region, then increasing steadily until L6. For the VBHv, the maximum value was found at the level of L6 and the smallest at the level of T7. At the level of T10, VBHd and VBHv had a similar value. In the lumbar region, VBHd became larger than VBHv, as much as 1.8 mm. DT ranged between 1.3 and 2.1 mm in the thoracic region, while in the lumbar region it showed greater values ranging between 2.6 and 3.3 mm. It was as much as 1.6 mm thicker in the lumbar than in the thoracic spine. Statistically significant differences ($P<0.0001$) were observed in VBHd, VBHv and DT between the vertebral levels from T2 to L6. At L6 level the maximum value of VBW was observed and the minimum at T8. The minimum value of WBD was found at T12 level and the maximum at T8. The vertebral body was wider than it was deep over the whole thoracolumbar spine, which was most obvious in the lumbar vertebrae. CBT showed the maximum value at T2 and the minimum at T5. There was no significant difference in VBW, VBD and CBT between the vertebral levels. The vertebral body and intervertebral disc measurements are listed in Table 2.

The spinal canal was the widest at T2 in the thoracic region, then narrowing at T10 and increasing again in the lumbar region to reach the maximum width over the entire thoracolumbar spine at L6. SCD showed the maximum value at T2; then decreasing slightly at T10, thereafter increasing at L6. In the lumbar region SCW was as much as 5.4 mm larger than SCD, while the mid thoracic region showed the smallest spinal canal dimensions over the entire thoracolumbar region. The spinal canal showed a trend similar to the vertebral body, which was wider than it was deep over the whole thoracolumbar spine. L1 was exceptionally different, the canal width and depth being equal. TPL decreased slightly from T2 to T12 and then reached the maximum value at level L5. The previous parameters are

listed in Table 3. There were significant differences (P<0.0001) in previous parameters between the vertebral levels.

Pedicle parameters are shown in Table 4. PDW ranged from 4.6 to 8.4 mm and showed an increase from the cranial thoracic spine toward the caudal level lumbar vertebrae reaching the maximum value at L5. PDH showed the lowest value at T2, while the highest value was observed at L5. PAL ranged between 26.7 and 37.1 mm. T7 showed the maximum value in the thoracic region, then decreasing caudally at T12, which was the shortest length in the thoracolumbar spine, and increased again until L3. PAA decreased from T2 to T8, thereafter increasing until T11, and decreased again at level of T13. In the lumbar region, PAA showed a constant increase, reaching the maximum value in the whole of the thoracolumbar spine at L6. TPA was the greatest at T12 level, decreasing caudally to this level until L6, while the lowest value over the whole thoracolumbar spine was observed at level T6. However, a significant (P<0.0001) difference was observed in all pedicle parameters between the vertebral levels.

Discussion

Human spines are difficult to obtain fresh and in large quantities for in vitro studies. Therefore, animal spines represent a suitable alternative. Sheep are claimed to be one of the most representative animal models for orthopaedic research [24] and precise morphometrical data are needed when sheep are used as a model for orthopaedic spinal research. The present study, therefore, provided CT reference values for the thoracolumbar spine of healthy sheep.

A variety of animal species have been used as model for human orthopaedic studies. Martini et al. [24] compared the sheep to the other available animal models for human orthopaedic researches. They reported nonhuman primates provide an excellent model thanks to their analogy with humans, but are not cost-efficient, require stringent controls and could cause severe zoonotic diseases, as well as the ethical pressures of using this species. In spite the physiological similarity between human and pigs there are some problems limiting their use such as rapid body growth and weight which affect the long term orthopaedic studies. Small pig breeds can be used to minimize the previous problems but they are more expensive and sometimes difficult to recruit [24]. Because of the previously mentioned considerations, sheep are becoming popular as animal models in orthopaedic research. Furthermore, sheep are quite similar in body weight to humans, and sufficiently large to allow serial sampling and multiple experimental procedures. Wilke et al. [28] compared the quantitative biomechanical properties of the sheep spine to human and concluded there are biomechanical similarities of

sheep and human spines and the sheep spine can serve as model for the evaluation of spinal implants.

To obtain uniformity, the animals were of equal age, weight, sex and breed. The number of 5 animals used was the lowest possible to comply with the rules of 3R but sufficient enough to provide reliable data [5-8]. Sheep in the present study were female because osteoporosis studies are most commonly conducted on female gender.

It could be argued that the number of sheep spines used was small. In order to overcome the problem of a small sample size, significance for analysis was set using a low p value (P<0.0001). However, the nearly similar sheep dimensions and small variance around the mean indicated that a larger sample size was not necessary. Moreover, previous investigators had used comparable sample sizes for similar studies [25-29].

CT is the examination of choice for assessing the bony structures of the spine. The perceived image quality depends on the choice of imaging parameters and also on the post-processing, in particular the reconstruction algorithm and the reformatting parameters, as well as the mode of display [30].

Dorsal recumbency is the position of choice for spine CT imaging, because it ensures minimal respiratory movements of the spine. In our study, sheep were positioned in sternal recumbency for two reasons: Firstly, with sternal recumbency, we could mimic the natural position of the spine as much as possible, particularly the kyphosis in lumbar spine. Secondly, this was performed to minimise the complications of general anaesthesia [31]. Short tube rotation time (0.75 second) setting was used to minimise the influence of respiratory movements on image quality [32,33].

Slice thickness affects an image's quality through its influence on spatial resolution. However, thin slice thickness reduces the amount of volume averaging and thus improves spatial resolution. For orthopaedic imaging, scanning with thin-slice collimation is preferable, ideally 1.5 mm or less [30], Therefore, slice thickness in the current study was less than 1.5 mm. Decreasing slice thickness increases the image noise. To keep the noise at an acceptable level, high mA and wide window display should be used [32,33]. In the present study, therefore, CT scanning setting was 200 mA and 2000 Hounsfield units window width. These settings, moreover, are consistent with published spinal CT imaging protocol [33].

Pitch describes the relationship between the table increment during one full gantry rotation and the slice thickness [32,33]. Pitch is directly proportional to image blur. Therefore, a highly pitched CT scan results in a very blurry image. The pitch has to be less than 2 for orthopaedic imaging, which is often chosen significantly lower than this, around 0.3-0.5 for

multi-slice CTs [30]. In this study, the pitch setting was within the aforementioned range (0.438).

The picture archiving and communication system instrumentation permits manipulation of the CT data, with adjustment of contrast for optimisation of image quality and measurement of distance, area and angle. Nevertheless, potential sources of error remain. One source of error is the accurate identification of precise anatomical points [23]. Intra-observer tests were carried out to analyse the magnitude of such errors. We found that the intra-observer error was within the limit of 5% [34]. Inter-observer error was not assessed, as all measurements for this database were performed by a single observer in order to maximise the CT measurement accuracy [22].

The results of the current study showed that the vertebral bodies were wider than deep, most obviously in the lumbar vertebrae. The spinal canal has a similar behaviour like vertebral bodies, while it tends to have nearly an equal width and depth at the caudal thoracic region. The intervertebral discs were thicker in the lumbar than in the thoracic spine. The pedicles were higher and longer than they were wide over the entire thoracolumbar spine.

We are aware of the elaborate work done by Wilke and co-workers [29]. They studied the anatomical dimensions of the vertebral body, pedicle, spinal canal, spinous and transverse processes, and articular facet and intervertebral disc for comparison with human data. Their database provides information regarding the anatomy of three- to four-year-old sheep.

There is agreement between their results and our findings. However, the measurements of the previous study tended to be 1.4-5.9 times larger than the present study. The causes of the difference could be attributed to age variation, as we used a 2-year-old sheep, and measuring methods. Wilke et al. [29] used a manual measurement method on the cadaveric spine, while we used CT. The manual measurements based on Vernier caliper were rounded to the nearest millimetre, which represents a potential measurement error of the order of 6-7% in measurements. Moreover, the irregular shape of the bony surfaces may induce some variability and or error when determining the dimensions of the vertebra [35,36].

In contrast to a previous study [29] the current study was carried out on live subjects and thus the influences of preservation methods on actual dimensions were excluded. Some parameters, such as PDL, PAL and PAA, have been reported here for the first time in sheep thoracolumbar spine. Therefore, it should be considered inevitable that sheep are used as a model for spinal fixation research [16].

The comparative biomechanical characteristics of the sheep were presented elsewhere [28]. We did not test the biomechanical properties of sheep spinal segments as this was not the

aim of our study. However, the current results could be interpreted from a biomechanical perspective.

A previous study carried out on ovine spine stated that the dorsoventral movement was the highest at the L6 level [28]. The vertebral body shape has an influence on the spinal movements. However, the horizontal oval shape of the vertebral body facilitates the dorsoventral movements [37]. In our study L6 had the most horizontal oval vertebral body over the whole of the thoracolumbar spine, which can explain the observation of the highest range of dorsoventral movement at this level.

In humans, spinal canal dimensions have an influence on spine dorsoventral movement, where greater spinal canal dimensions facilitate the flexion motion [38,39]. In the current study, the spinal canal dimensions were the greatest at L6 and the lowest at T10. Based on these results, we expect the highest flexion to be at L6 and the lowest at T10. A biomechanical study carried out on sheep spine revealed that flexion was the highest at the L6 level (5.29°±0.82) and the lowest at T10 (1.93°±0.3) [28], which confirms our expectations.

In humans, the pedicle represents a stronger site for screw placement than the vertebral body. The trabeculae in the pedicle appear to be thicker and stronger. Moreover, the pedicle cortex is thicker allowing the screw threads to engage with cortical bone [16]. Pedicle morphometry plays an important role in transpedicular screw fixation, because it is related to screw placement [16]. The diameter of the screw should be 80% or less of the diameter of the pedicle [23]. Therefore, the current study presents the needed precise morphometrical data for using sheep as a model for transpedicular fixation research.

It was interesting to note that the PDW increased from cranial thoracic spine to caudal level lumbar vertebrae. PDW determines the diameter of appropriate transpedicular screws, the wider pedicle allowing the use of a thicker screw, which provides greater fixation.

No previous studies quantitatively measured PAL, PDL and PAA in the thoracolumbar spine of sheep, knowledge of which is important for transpedicular screw placement and prevention of perforation of the ventral aspect of the cortex by the screws and injury to vital structures.

PDL and PAL defined the minimum and maximum length of screw needed to obtain a grip on the entire pedicle, respectively. In our study, PDL was as much as 29.2-53.0% of PAL. Thus, a transpedicular screw length should be at least 53.0% of PAL. PAA may be an important parameter for correct pedicle screw placement. In humans, Louis [40] and Roy-Camille et al. [41] recommend that a pedicle screw should be inserted in a straight (vertical) direction. In

contrast, Krag et al. [16] and Zindrick et al. [42] believe that insertion of the pedicle along the medial trajectory is a safer technique. Jahng et al. [43] reported in their experiments on sheep lumbar spine that there is a noticeable difference between the TPA and PAA, which is consistent with the current results. The difference between the TPA and PAA is most likely due to the different vertebral types (type I or II). Therefore, we predict a high misplacement rate when a pedicle screw is inserted in a straight direction.

In the lumbar region, DT was as much as 57.4% thicker than those in the thoracic vertebrae. A thicker disc provides more mobility than a thinner one [44]. In contrast, transverse processes were longer in the lumbar than in the thoracic region, which can explain the restriction of lateral bending and axial rotation in the lumbar compared to the thoracic region [28].

A limitation of this study could be the accuracy of the small measurement such as thickness of the cortical bone (less than 2 mm). This questionable, due to the influence of the volume averaging artefact. Therefore, a thin slice thickness was set to minimise the volume averaging effect.

In conclusion, this study provided a comprehensive quantitative database of the normal sheep thoracolumbar spine. This descriptive information can be used to help determine whether the sheep spine can be a representative model for testing a certain application. When testing new implants and surgical techniques, i.e. intrapedicular screw, scaling differences should be taken into account to select the suitable implants' size for application.

Footnotes

None of the authors have any financial or personal relationships with individuals or organisations that could inappropriately influence the content of this paper.

References

1. Wilke HJ, Wenger K, Claes L. Testing criteria for spinal implants: recommendations for the standardization of in vitro stability testing of spinal implants. Eur Spine J. 1998;7(2):148–154.

2. Goel VK, Panjabi MM, Patwardhan AG, Dooris AP, Serhan H. American Society for Testing and Materials. Test protocols for evaluation of spinal implants. J Bone Joint Surg Am. 2006;88(Suppl 2):103–109.

3. Ashman RB, Bechtold JE, Edwards WT, Johnston CE, 2nd, McAfee PC, Tencer AF. In vitro spinal arthrodesis implant mechanical testing protocols. J Spinal Disord. 1989;2(4):274–281.

4. Tominaga T, Dickman CA, Sonntag VK, Coons S. Comparative anatomy of the baboon and the human cervical spine. Spine. 1995;20(2):131–137.

5. Smit TH. The use of a quadruped as an in vivo model for the study of the spine - biomechanical considerations. Eur Spine J. 2002;11(2):137–144.

6. Edmondston SJ, Singer KP, Day RE, Breidahl PD, Price RI. Formalin fixation effects on vertebral bone density and failure mechanics: an in-vitro study of human and sheep vertebrae. Clin Biomech (Bristol, Avon) 1994;9(3):175–179.]

7. Eggli S, Schläpfer F, Angst M, Witschger P, Aebi M. Biomechanical testing of three newly developed transpedicular multisegmental fixation systems. Eur Spine J. 1992;1(2):109–116.

8. Gurwitz GS, Dawson JM, McNamara MJ, Federspiel CF, Spengler DM. Biomechanical analysis of three surgical approaches for lumbar burst fractures using short-segment instrumentation. Spine.1993;18(8):977–982.

9. Yoganandan N, Kumaresan S, Voo L, Pintar FA. Finite element applications in human cervical spine modeling. Spine (Phila Pa 1976) 1996;21(15):1824–1834.

10. Kiefer A, Shirazi-Adl A, Parnianpour M. Stability of the human spine in neutral postures. Eur Spine J. 1997;6(1):45–53.

11. Newman E, Turner AS, Wark JD. The potential of sheep for the study of osteopenia: current status and comparison with other animal models. Bone. 1995;16(4):277S–284S.

12. Nunamaker DM. Experimental models of fracture repair. Clin Orthop Relat Res. 1998;355:S56–S65.

13. Bergmann G, Graichen F, Rohlmann A. Hip joint forces in sheep. J Biomech. 1999;32(8):769–777.

14. Egermann M, Goldhahn J, Schneider E. Animal models for fracture treatment in osteoporosis.Osteoporos Int. 2005;16:S129–S138.

15. Turner AS. Experiences with sheep as an animal model for shoulder surgery: strengths and shortcomings. J Shoulder Elbow Surg. 2007;16(5):S158–S163.

16. Krag MH, Weaver DL, Beynnon BD, Haugh LD. Morphometry of the thoracic and lumbar spine related to transpedicular screw placement for surgical spinal fixation. Spine. 1988;13(1):27–32.

17. Olsewski JM, Simmons EH, Kallen FC, Mendel FC, Severin CM, Berens DL. Morphometry of the lumbar spine: anatomical perspectives related to transpedicular fixation. J Bone Joint Surg Am.1990;72(4):541–549.

18. Abuzayed B, Tutunculer B, Kucukyuruk B, Tuzgen S. Anatomic basis of anterior and posterior instrumentation of the spine: morphometric study. Surg Radiol Anat. 2010;32(1):75–85.

19. Kadioglu HH, Takci E, Levent A, Arik M, Aydin IH. Measurements of the lumbar pedicles in the Eastern Anatolian population. Surg Radiol Anat. 2003;25(2):120–126.

20. Wolf A, Shoham M, Michael S, Moshe R. Morphometric study of the human lumbar spine for operation-workspace specifications. Spine. 2001;26(22):2472–2477.

21. Way TW, Chan HP, Goodsitt MM, Sahiner B, Hadjiiski LM, Zhou C, Chughtai A. Effect of CT scanning parameters on volumetric measurements of pulmonary nodules by 3D active contour segmentation: a phantom study. Phys Med Biol. 2008;53(5):1295–1312.

22. Beers GJ, Carter AP, Leiter BE, Tilak SP, Shah RR. Interobserver discrepancies in distance measurements from lumbar spine CT scans. Am J Roentgenol. 1985;144(2):395–398.

23. Zhou SH, McCarthy ID, McGregor AH, Coombs RR, Hughes SP. Geometrical dimensions of the lower lumbar vertebrae--analysis of data from digitised CT images. Eur Spine J. 2000;9(3):242–248.

24. Martini L, Fini M, Giavaresi G, Giardino R. Sheep model in orthopedic research: a literature review.Comp Med. 2001;51(4):292–299.

25. Kumar N, Kukreti S, Ishaque M, Mulholland R. Anatomy of deer spine and its comparison to the human spine. Anat Rec. 2000;260(2):189–203.

26. McLain RF, Yerby SA, Moseley TA. Comparative morphometry of L4 vertebrae: comparison of large animal models for the human lumbar spine. Spine (Phila Pa 1976) 2002;27(8):E200–E206.

27. Riley LH, 3rd, Eck JC, Yoshida H, Koh YD, You JW, Lim TH. A biomechanical comparison of calf versus cadaver lumbar spine models. Spine. 2004;29(11):E217–E220.

28. Wilke HJ, Kettler A, Claes LE. Are sheep spines a valid biomechanical model for human spines?Spine. 1997;22(20):2365–2374.

29. Wilke HJ, Kettler A, Wenger KH, Claes LE. Anatomy of the sheep spine and its comparison to the human spine. Anat Rec. 1997;247(4):542–555.

30. Tins B. Technical aspects of CT imaging of the spine. Insights imaging. 2010;1(5-6):349–359.

31. Mitchell B, Williams J. Respiratory function changes in sheep associated with lying in lateral recumbency and with sedation by xylazine. Vet Anaesth Analg. 1976;6(1):30–36.

32. Schwarz T, Saunders J. CT acquisitation principle. In: Schwarz T, Saunders J, editors. Veterinary computed tomography. 1st ed. Oxford: Wiley-Blackwell; 2011. pp. 9–27.

33. Seiler G, Kinns J, Dennison S, Saunders J, Schwarz T. Vertebral column and spinal cord. In: Schwarz T, Saunders J, editors. Veterinary computed tomography. 1st ed. Oxford: Wiley-Blackwell; 2011. pp. 209–228.

34. Bland JM, Altman DG. Statistical methods for assessing agreement between two methods of clinical measurement. Lancet. 1986;1(8476):307–310.

35. Flynn JR, Bolton PS. Measurement of the vertebral canal dimensions of the neck of the rat with a comparison to the human. Anat Rec. 2007;290(7):893–899.

36. Tatarek NE. Variation in the human cervical neural canal. Spine J. 2005;5(6):623–631.

37. Denoix JM. Spinal biomechanics and functional anatomy. Vet Clin North Am Equine Pract.1999;15(1):27–60.

38. Schönström N, Lindahl S, Willén J, Hansson T. Dynamic changes in the dimensions of the lumbar spinal canal: an experimental study in vitro. J Orthop Res. 1989;7(1):115–121.

39. Inufusa A, An HS, Lim TH, Hasegawa T, Haughton VM, Nowicki BH. Anatomic changes of the spinal canal and intervertebral foramen associated with flexion-extension movement. Spine.1996;21(21):2412–2420.

40. Louis R. Fusion of the lumbar and sacral spine by internal fixation with screw plates. Clin Orthop Relat Res. 1986;203:18–33.

41. Roy-Camille R, Saillant G, Mazel C. Internal fixation of the lumbar spine with pedicle screw plating.Clin Orthop Relat Res. 1986;203:7–17.

42. Zindrick MR, Wiltse LL, Doornik A, Widell EH, Knight GW, Patwardhan AG, Thomas JC, Rothman SL, Fields BT. Analysis of the morphometric characteristics of the thoracic and lumbar pedicles. Spine.1987;12(2):160–166.

43. Jahng TA, Fu TS, Kim DH. Open versus endoscopic lumbar pedicle screw fixation and posterolateral fusion in a sheep model: a feasibility study. Spine J. 2004;4(5):519–526.

44. Haussler KK. Anatomy of the thoracolumbar vertebral region. Vet Clin North Am Equine Pract.1999;15(1):13–26.

Table 1 Mean of coefficient of variation (CV) values of thoracolumbar spine measurements of healthy Merino-sheep

Dimension	Abbreviations	Mean CV %
Vertebral body width	VBW	1.5 ± 0.6
Vertebral body depth	WBD	1.3 ± 0.6
Dorsal vertebral body height	VBHd	1.5 ± 0.4
Ventral vertebral body height	VBHv	2.1 ± 0.3
Cortical bone thickness	CBT	3.6 ± 0.6
Disc thickness	DT	2.5 ± 0.7
Spinal canal width	SCW	2.2 ± 1.0
Spinal canal depth	SCD	1.5 ± 0.1
Transverses process length	TPL	1.0 ± 0.6
Pedicle width	PDW	1.7 ± 1.0
Pedicle height	PDH	1.4 ± 0.5
Pedicle axis length	PAL	1.5 ± 0.8
Pedicle axis angle	PAA	1.9 ± 1.1
Pedicle length	PDL	1.1 ± 0.4
Transverse pedicle angle	TPA	2.8 ± 1.7

Table 2 Mean and standard deviation of CT measurements related to intervertebral disc and vertebral bodies of thoracolumbar spine of healthy Merino-sheep.

	DT (mm)	CBT (mm)	VBHv (mm)	VBHd (mm)	VBD (mm)	VBW (mm)
T2	2.1 ± 0.7^{a,b,c}	2.3 ± 1.8	24.8 ± 1.0^{a}	25.0 ± 1.1^{a}	17.0 ± 0.9	26.7 ± 0.9
T3	1.9 ± 0.6^{a,b,c}	1.3 ± 0.3	26.7 ± 1.3^{a,c}	24.1 ± 3.9^{a,c}	17.0 ± 0.7	25.4 ± 1.1
T4	1.5 ± 0.3^{a,c}	1.4 ± 0.3	26.5 ± 0.7^{a,c}	25.6 ± 1.6^{a,d}	16.4 ±0.9	24.8 ± 1.6
T5	1.5 ± 0.3^{a,c}	1.2 ± 0.4	25.7 ± 0.7^{a,c}	26.4 ± 1.3^{a,c,d}	16.5 ± 1.6	24.0 ± 0.9
T6	1.3 ± 0.3^{a}	1.3 ± 0.4	26.2 ± 2.2^{a,c}	25.0 ± 0.3^{a,c}	16.6 ± 1.5	24.4 ± 0.8
T7	1.6 ± 0.3^{a,c}	1.3 ± 0.4	24.5 ± 0.7^{a,d}	24.2 ± 1.0^{a,c}	16.9 ± 1.3	24.6 ± 0.5
T8	1.5 ± 0.1^{a,c}	1.3 ± 0.5	25.5 ± 1.1^{a,d}	24.9 ± 0.7^{a,c}	18.5 ± 3.3	22.7 ± 2.8
T9	1.6 ± 0.3^{a,c}	1.4 ± 0.2	25.7 ± 0.6^{a,c,d}	26.2 ± 0.8^{a,c}	17.3 ± 1.1	24.8 ± 2.7
T10	1.5 ± 0.1^{a,c}	1.4 ± 0.3	27.2 ± 1.5^{a,c,d,e}	27.2 ± 1.1^{a,c,d,e}	16.6 ± 1.1	23.2 ± 1.6
T11	1.6 ± 0.1^{a,c}	1.5 ± 0.4	28.2 ± 4.0^{a,c,d,e}	30.4 ± 2.6^{a,b,c,d,e}	16.7 ± 1.5	24.6 ± 2.0
T12	1.6 ± 0.3^{a,c}	1.5 ± 0.3	29.7 ± 2.0^{a,b,c,d,e}	30.3 ± 2.5^{a,b,c,d,e}	16.1 ± 1.3	30.3 ± 5.3
T13	1.8 ± 0.2^{a,b,c}	1.4 ± 0.1	32.5 ± 2.0^{b,c,d}	33.0 ± 1.8^{b,c,d}	16.5 ± 1.7	28.0 ± 3.3
L1	3.3 ± 1.0^{b,c}	1.8 ± 0.6	34.2 ± 0.5^{b,c,d}	36.2 ± 0.8^{b,d}	18.3 ± 0.8	24.5 ± 2.2
L2	2.6 ± 0.5^{a,b,c}	1.4 ± 0.3	35.3 ± 1.1^{b,c,d}	37.6 ± 0.8^{b,e}	17.7 ± 1.1	23.7 ± 3.6
L3	2.6 ± 0.5^{a,b,c}	1.5 ± 0.5	36.2 ± 0.5^{b,c}	38.4 ± 1.0^{b}	18.0 ± 1.9	24.4 ± 2.7
L4	2.7 ± 0.5^{a,b,c}	1.4 ± 0.5	37.4 ± 0.6^{b,e}	39.2 ± 0.9^{b}	17.9 ± 2.2	24.0 ± 3.1
L5	2.9 ± 0.5^{a,c}	1.5 ± 0.2	38.9 ± 0.3^{b,e}	39.9 ± 1.9^{b}	17.1 ± 2.1	24.7 ± 2.6
L6	2.9 ± 0.3^{a,c}	1.4 ± 0.2	38.7 ± 2.9^{b,e}	40.7 ± 1.0^{b}	16.3 ± 1.7	32.0 ± 7.3
F	10.042*	0.873 $^{N.S.}$	16.816*	22.664*	1.005 $^{N.S.}$	3.304 $^{N.S.}$

* $P < 0.0001$; N.S., not significant; different superscript letters in the same column are significantly different ($P < 0.0001$).DT, disc thickness; CBT, cortical bone thickness; VBHv, vertebral body height ventral; VBHd, vertebral body height dorsal; VBW, vertebral body Width; VBD, vertebral body depth.

Table 3 Mean and standard deviation of CT measurements dimensions related to spinal canal and transverse processes of thoracolumbar spine of healthy Merino-sheep.

	SCW (mm)	SCD (mm)	TPL (mm)
T2	15.6 ± 1.0^{a,b,c}	12.4 ± 0.9^{a}	51.7 ± 2.4^{a}
T3	14.5 ± 0.3^{a}	10.9 ± 0,7^{a,b}	47.2 ± 2.0^{a}
T4	13.7 ± 0.5^{a}	10.9 ± 0.4^{a,b}	45.8 ± 2.5^{a}
T5	13.3 ± 1.6^{a}	11.0 ± 1.3^{a,b}	43.9 ± 2.1^{a}
T6	11.8 ± 0.5^{a,b}	10.5 ± 0.8^{a,b}	40.2 ± 4.2^{a}
T7	11.8 ± 0.5^{a}	10.5 ± 1.1^{a,b}	42.8 ± 2.1^{a}
T8	11.9 ± 0.6^{a}	9.8 ± 0.6^{a,b}	45.2 ± 2.8^{a}
T9	11.9 ± 0.6^{a}	9.6 ± 0.4^{a,b}	46.7 ± 2.4^{a}
T10	11.6 ± 0.3^{a}	9.4 ± 0.6^{b}	47.3 ± 2.3^{a}
T11	12.2 ± 0.5^{a}	9.5 ± 0.6^{b}	49.8 ± 6.8^{a}
T12	13.3 ± 0.6^{a,c}	9.5 ± 0.5^{a,b}	49.0 ± 3.7^{a}
T13	13.2 ± 0.9^{a,c}	9.4 ± 0.8^{b}	55.9 ± 3.3^{c,b}
L1	9.8 ± 0.6^{a,c}	9.8 ± 0.7^{a,b}	94.2 ± 9.2^{c}
L2	14.4 ± 0.4^{a,c}	10.4 ± 1.1^{a,b}	116.4 ± 10.3^{b,c}
L3	15.2 ± 1.1^{a,b,c}	10.0 ± 1.2^{a,b}	123.4 ± 11.7^{b}
L4	15.2 ± 3.3^{a,b,c}	10.2 ± 1.0^{a,b}	128.6 ± 10.6^{b}
L5	16.9 ± 1.2^{b,c}	10.7 ± 1.0^{a,b}	130.9 ± 10.6^{b}
L6	18.9 ± 1.6^{b,c}	12.2 ± 0.7^{a,b}	127.3 ± 7.8^{b}
F	14.626*	5.501*	195.274*

$^{*}P$< 0.0001; N.S. not significant; different superscript letters in the same column are significantly different (P < 0.0001). SCW, spinal canal width; SCD, spinal canal depth; TPL, transverse process length.

Table 4 Mean and standard deviation of CT measurements dimensions and angels related to pedicles of five Merino-sheep thoracolumbar spine.

	PDW (mm)	PAL (mm)	PAA (°)	PDL (mm)	PDH (mm)	TPA (°)
T2	4.6 ± 2.9^{a}	31.1 ± 4.3^{a,b}	26.3 ± 1.9^{a,b}	10.9 ± 1.1^{a}	12.0 ± 1.2^{a,c,d}	15.9 ± 9.3^{a,b,c}
T3	5.0 ± 0.7^{a,b}	28.6 ± 1.7^{a,b}	25.1 ± 2.5^{a}	9.7 ± 0.9^{a,b}	13.0 ± 1.9^{a,c,d}	7.2 ± 5.5^{a,b}
T4	6.2 ± 1.9^{a,b}	31.9 ± 4.5^{a,b}	24.5 ±1.3^{a}	10.4 ± 0.5^{a,b}	13.6 ± 0.9^{a}	7.2 ± 4.8^{a}
T5	6.2 ± 0.8^{a,b}	33.0 ± 4.6^{a,b}	24.1 ± 1.2^{a}	10.8 ± 1.4^{a,b}	13.6 ± 0.5^{a,c}	5.5 ± 1.7^{a}
T6	6.7 ± 1.1^{a,b}	33.5 ± 3.8^{a,b}	23.5 ± 1.9^{a}	12.1 ± 1.3^{a,b}	13.5 ± 1.2^{a}	4.36 ± 3.4^{a}
T7	7.0 ± 0.9^{a,b}	35.0 ± 2.1^{a,b}	23.6 ± 1.9^{a}	12.3 ± 2.0^{a,b}	14.0 ± 1.1^{a}	5.7 ± 4.5^{a}
T8	7.2 ± 0.9^{a,b}	34.8 ± 1.5^{a,b}	22.6 ± 1.4^{a}	11.7 ± 0.9^{a,b}	14.4 ± 1.3^{a}	7.0 ± 3.6^{a,b}
T9	6.7 ± 0.6^{a,b}	33.8 ± 1.4^{a,b}	23.6 ± 1.4^{a}	11.1 ± 1.0^{a,b}	16.2 ± 1.1^{a}	6.4 ± 5.3^{a}
T10	7.0 ± 0.5^{a,b}	31.2 ± 2.4^{a,b}	25.1 ± 1.3^{a}	11.9 ± 0.9^{a,b}	17.8 ± 2.0^{a,c}	9.4 ± 5.4^{a}
T11	7.8 ± 0.8^{a,b}	28.8 ± 1.9^{a,b}	26.8 ± 2.4^{a,b}	12.2 ± 0.7^{a,b}	18.5 ± 1.4^{a,c,d}	23.0 ± 3.4^{a}
T12	6.3 ± 1.9^{a,b}	26.7 ± 2.2^{a}	23.6 ± 4.4^{a}	13.6 ± 1.9^{a,b}	19.3 ± 1.8^{c}	28.6 ± 3.0^{c}
T13	5.2 ± 0.5^{a,b}	30.4 ± 3.7^{a,b}	22.1 ± 1.0^{a}	16.1 ± 3.0^{b}	23.1 ± 3.5^{b,c}	21.0 ± 4.4^{a,b,c}
L1	6.0 ± 1.0^{a,b}	33.6 ± 4.0^{a,b}	22.4 ± 1.3^{a}	13.1 ± 2.6^{a,b}	23.9 ± 3.3^{b,c}	17.3 ± 7.4^{a,b,c}
L2	7.3 ± 0.6^{a,b}	36.1 ± 1.5^{a,b}	24.7 ± 0.8^{a}	11.2 ± 0.9^{a,b}	27.9 ± 1.3^{b}	21.1 ± 3.6^{a,b,c}
L3	7.7 ± 1.6^{a,b}	37.1 ±1.1^{b}	25.7 ± 1.5^{a}	11.3 ± 1.8^{a,b}	28.8 ± 1.3^{b}	18.5 ± 2.5^{a,b,c}
L4	8.2 ± 0.7^{a,b}	36.7 ± 1.9^{b}	26.5 ± 1.2^{a,b}	11.3 ± 0.9^{a,b}	27.5 ± 1.4^{b}	19.0 ± 3.8^{a,b,c}
L5	8.4 ± 0.5^{b}	36.5 ± 1.2^{a,b}	27.5 ± 0.8^{a,b}	12.9 ± 2.6^{a,b}	29.0 ± 1.5^{b}	15.5 ± 2.5^{a,b,c}
L6	8.3 ± 1.6^{b}	35.2 ± 2.8^{a,b}	32.0 ± 1.7^{b}	12.1 ± 2.1^{a,b}	27.2 ± 1.9^{b}	12.5 ± 4.3^{a,b,c}
F	4.377*	5.734*	7.929*	3.151*	63.169*	12.141*

$^{*}P$ < 0.0001; N.S., not significant; different superscript letters in the same column are significantly different (P < 0.0001). PDW, pedicle width; PAL, pedicle axis length; PAA, pedicle axis angle; PDL, pedicle length; PDH, pedicle height; TPA, transverse pedicle angle.

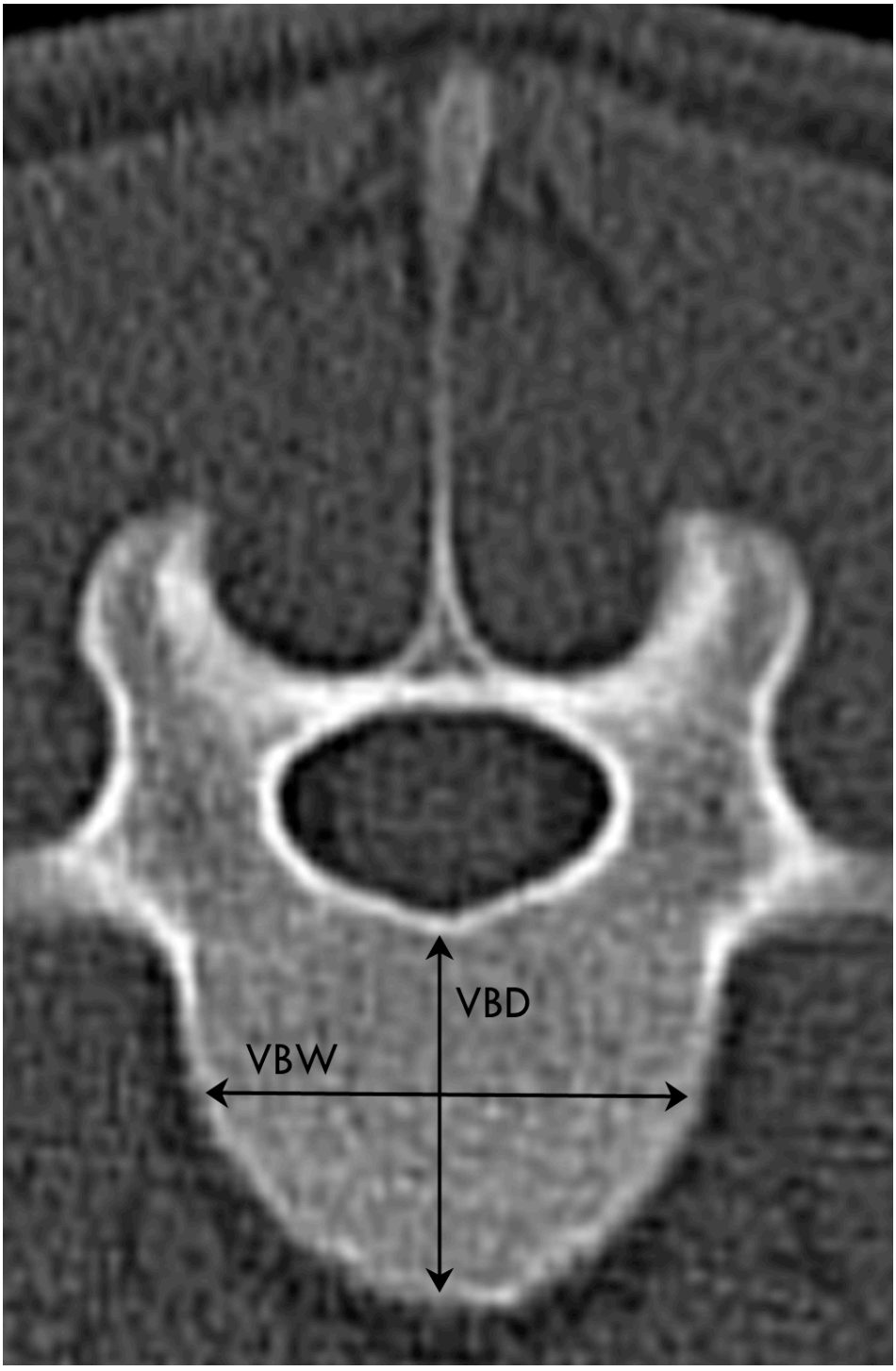

Figure 1. Transverse CT image obtained at the cranial aspect of L5 of a 2-year-old clinically normal female Merino sheep illustrating the measurements obtained for T2 through L6. Left is right. The measurements of interest obtained for each of the thoracolumbar vertebrae were vertebral body width (VBW; widest distance between the lateral borders of the vertebral body), and vertebral body depth (VBD; distance between dorsal and ventral borders of vertebral body).

Figure 2. Sagittal CT image with measurements on the T9 in a two-year-old female Merino sheep illustrating vertebral body height at dorsal border (VBHd; distance between the most dorsocranial and the most dorsocaudal point of the same vertebral body), vertebral body height at ventral border (VBHv; distance between the most ventrocranial and the most ventrocaudal point of the same vertebral body) and disc thickness (DT; distance between cranial and caudal vertebral epiphyses of adjacent vertebrae). Cranial is to the left.

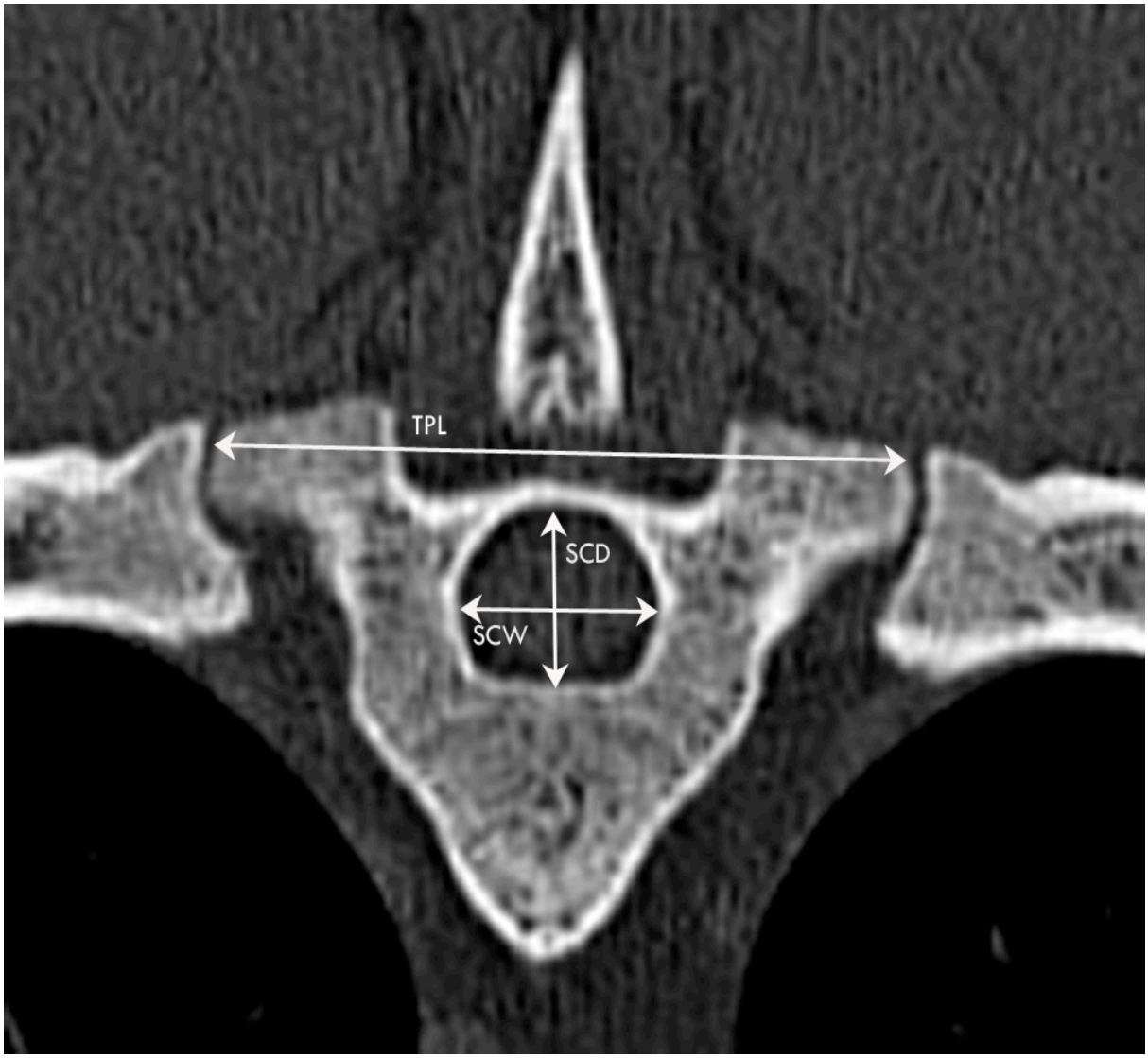

Figure 3. Transverse CT images obtained at the level of T7 of the same sheep as in Figure 1. Left is right. Spinal canal width (SCW; widest distance between axial cortices of pedicles), spinal canal depth (SCD; distance between dorsal border of vertebral body and lamina at vertebrae midline) and transverse process length (TPL; distance between tips of transverse processes).

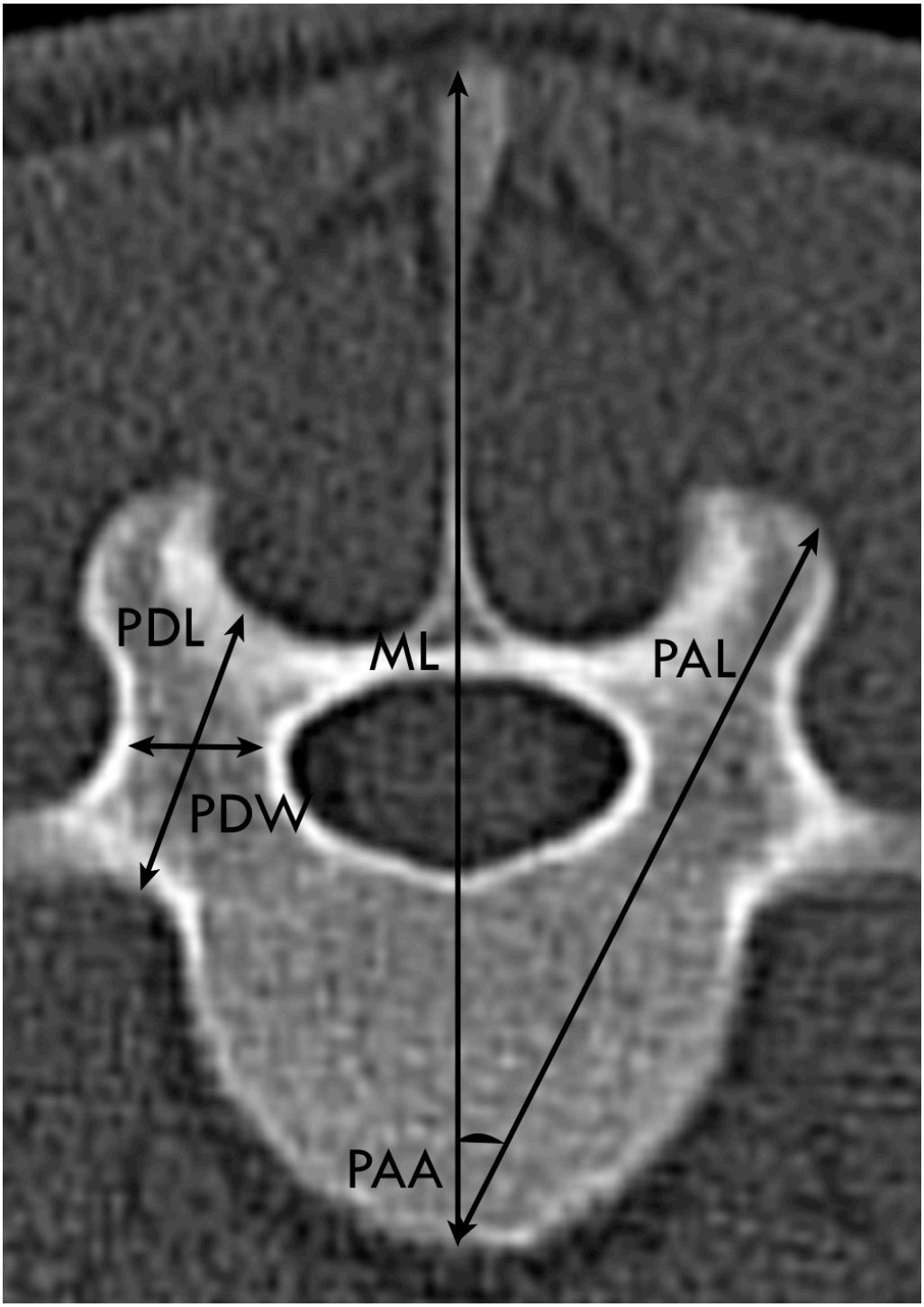

Figure 4. Transverse CT image obtained at the cranial aspect of L5 in a two-year-old female Merino sheep. Left is right. Pedicle length (PDL; distance between dorsal vertebral cortex and junction between ventral border of transverse process and vertebral body because of the vertebrae type II [the pedicle locates dorsal to the transverse process]), pedicle width (PDW;widest distance between the axial and abaxial border of pedicle), pedicle axis length (PAL; distance from dorsal vertebral lamina cortex to midpoint of ventral vertebral cortex,

pedicle axis angle (PAA; angle between PAL and vertebral midline) and sagittal midline (ML; line bisects the vertebrae to equal halves).

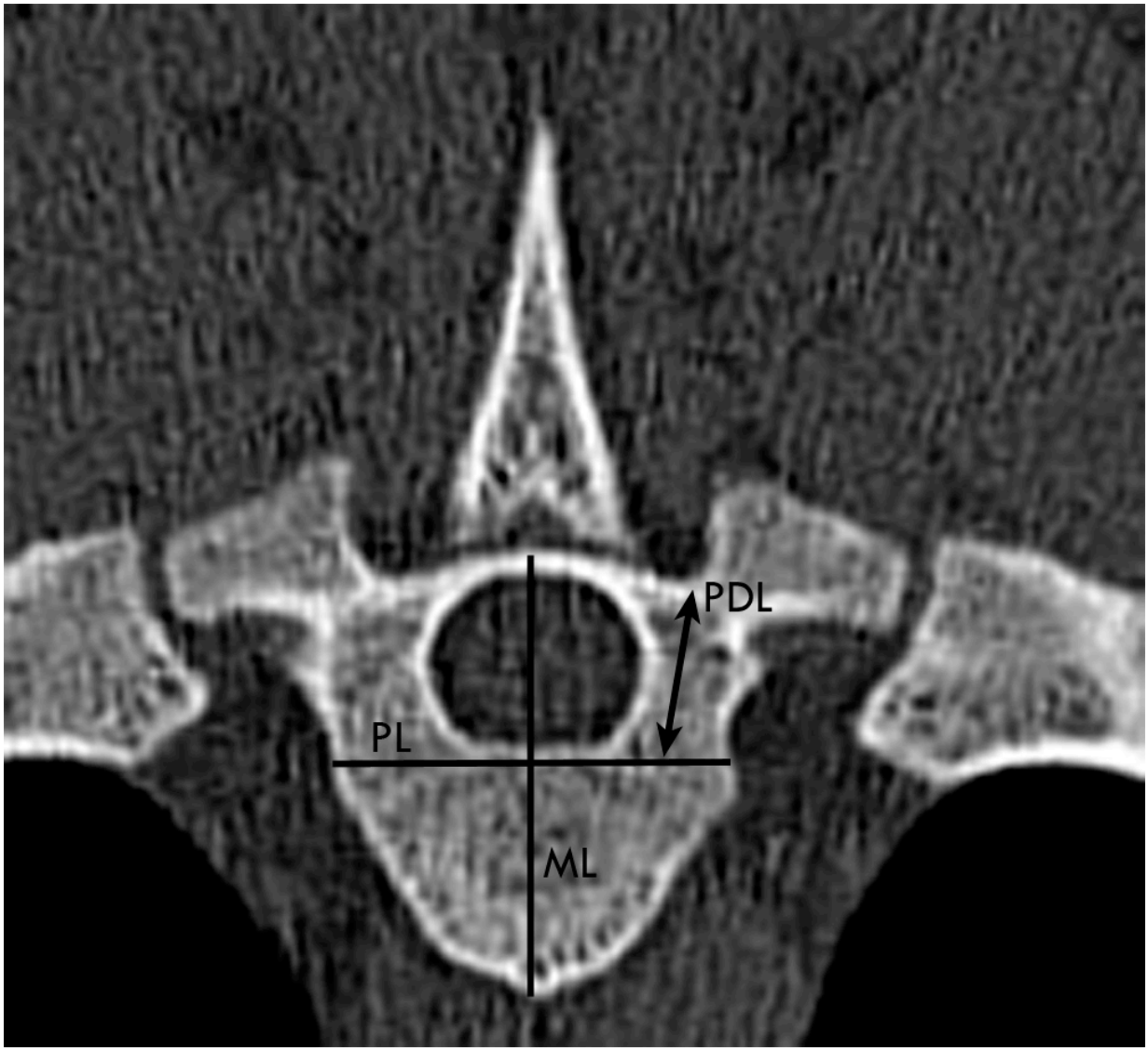

Figure 5. Transverse CT image obtained at the level of T5 vertebra in a two-year-old female Merino sheep. Left is right. Pedicle length (PDL; refers to pedicle type I, which islocated ventrally to the transverse process), sagittal midline (ML; line bisects the vertebrae to equal halves) and PL (perpendicular line to vertebral midline at the level of ventral border of the spinal canal).

3.2 Publication 2: Is sheep lumbar spine a suitable alternative model for human spinal researches? Morphometrical comparison study

Mahmoud Mageed[1,2*], Dagmar Berner[1], Henriette Jülke[3], Christian Hohaus[4], Walter Brehm[1], Kerstin Gerlach[1]

Laboratory animal research 2013 Dec;29(4):183-189.

http://dx.doi.org/10.5625/lar.2013.29.4.183

PMID: 24396382

[1]Large Animal Clinic for Surgery, Faculty of Veterinary Medicine, University of Leipzig, Leipzig, Germany.

[2]Department of Surgery and Anaesthesia, Faculty of Veterinary Medicine, University of Khartoum, Khartoum North, Sudan.

[3]Microsurgery and Animal Models Core, Translational Centre for Regenerative Medicine, University of Leipzig, Leipzig, Germany.

[4]Department of Neurosurgery, BG Hospital Bergmannstrost, Halle, Germany.

*Corresponding author: Mahmoud Mageed, Large Animal Clinic for Surgery, Faculty of Veterinary Medicine, University of Leipzig, An den Tierkliniken 21, D-04103, Leipzig, Germany. Tel: +49-341-9738264; Fax: +49-341-9738218; Email: mahmoud.mageed@hotmail.com

Received July 22, 2013

Revised September 03, 2013

Accepted September 12, 2013

Abstract

Sheep are commonly used as a model for human spinal orthopaedic research due to their similarity in morphological and biomechanical features. This study aimed to document the volumes of vertebral bodies and compare the generated results as well as morphometry of the sheep lumbar spine to human published data. For this purpose, computed tomography scans were carried out on five adult Merino sheep under general anaesthesia. Transverse 5 mm thick images were acquired from L1 to L6 using a multi-detector-row helical CT scanner. Volume measurements were performed with dedicated software. Four spinal indices and Pavlov's ratio were calculated. Thereafter, the generated data were compared to published literature on humans. The mean vertebral body volume showed an increase towards the caudal vertebrae, but there were no significant differences between the vertebral levels (P>0.05). Compared to humans, sheep vertebral body volumes were 48.6% smaller. The comparison of absolute values between both species revealed that sheep had smaller, longer and narrower vertebral bodies, thinner intervertebral discs, narrower spinal canal, longer transverse processes, shorter dorsal spinous processes and narrower, higher pedicles with more lateral angulations. The comparison of the spinal indices showed a good similarity to human in terms of the vertebral endplates and spinal canal. The results of this study may be helpful for using the sheep as a model for human orthopaedic spinal research if anatomical differences are taken into account.

Keywords: Comparative anatomy, human lumbar spine, spinal index, ovine, vertebral body volume.

Human lumbar vertebrae support the weight of the upper body. Moreover, they are the largest vertebrae in the dynamic part of the spinal column. Upright posture and locomotion cause significant loading stress to the vertebral bodies, which in turn predispose the lumbar spinal region to high incidence of spinal disorders such as herniated disc and spinal stenosis [1,2], and thus, new surgical procedures and spinal implants are developed and often tested pre-clinically on cadaver spines before being used in humans.

The human cadaveric spine is the ideal model for biomechanical studies and implant testing whenever anatomy and size are important. However, there are some difficulties in using the human model, such as obtaining it fresh especially from a healthy population and in large quantities in order to obviate the wide scattering effect associated with biological variability [3]. To overcome these obstacles, animal models such as sheep, calves, pigs and dogs have been used as alternatives for human spinal research [4-7].

Sheep are well accepted as appropriate models in orthopaedic research, due to similarities with humans in weight, bone and joint structure and in the bone remodelling processes [8-11]. In addition to their availability, ease of handling and housing, sheep are fully accepted as a research animal model in society [12].

Computed tomography (CT), a sensitive, non-invasive diagnostic and evaluating technique, has been used in morphometric studies to depict the normal volume and shape of the human vertebral canal at various levels [13-16]. Furthermore, via CT morphometric data could be obtained from a live subject, thus preventing the effect of preservation methods.

In humans, the exact volume of the vertebral body is necessary for the evaluation and surgical application related to vertebral body deformities such as vertebroplasty, in which an orthopaedic cement mixture is injected into the empty spaces within weakened vertebrae to strengthen them. Thereby, the vertebral body volume is crucial to decide the amount of the cement that should be injected into the deformed vertebra [15,16]. An animal model to test various compounds for vertebroplasty must be of sufficient size to accommodate realistic volumes of material. However, we have not found any detailed study in the literature describing the volumes of sheep lumbar vertebral bodies.

Morphometry of sheep lumbar vertebrae is essential for designing and interpreting results from studies which contemplate their use. In this study, we aimed to document the volumes of lumbar vertebral bodies and compare the volumes and morphometry of the sheep lumbar vertebrae to published data on humans.

Material and methods

This study was approved by the Animal Welfare Commission, Regional Office Leipzig (TVV-No. 03/12). Our study consisted of two parts; a volumetry of sheep lumbar vertebral bodies and a morphometric comparison study between the sheep and human lumbar vertebrae.

Determining the lumbar vertebral bodies' volume

For volumetric study, five female Merino sheep (mean age, 2±0.1 years; mean weight, 62±5.3 kg) without history or clinical signs related to spinal diseases were included.

Each sheep was fasted for 24 hours and deprived of water for 12 hours before being premedicated with 0.1 mg/kg atropine sulphate (Atropinum sulfuricum 0.5 mg Eifelango®, Eifelango, Bad Neuenahr-Ahrweiler, Germany), and a combination of 0.1 mg/kg butorphanol tartrate (Alvegesic®, CP-Pharma GmbH, Burgdorf, Germany) and 0.2 mg/kg midazolam (Midazolam, B. Braun; B.Braun, Melsung, Germany) administered intravenously. Anaesthesia was induced with 3 mg/kg ketamine chlorhydrate (Ursotamin®, Serumwerk Bernburg AG, Bernburg, Germany) intravenously. After endotracheal intubation, anaesthesia was maintained with isoflurane (Isofluran CP®, CP-Pharma GmbH) delivered in oxygen through an endotracheal tube.

The sheep were positioned in sternal recumbency and positioning aid tools were used to obtain a perpendicular position of the spine relative to the x-ray beam of the gantry. Contiguous slices were obtained from the cranial aspect of L1 to the caudal aspect of L6 with a multi-detector-row helical CT unit (Philips Medical Systems MX8000 IDT 16, Hamburg, Germany). Technical settings were 120 kV, 200 mA, 0.75 second tube rotation and a pitch of 0.438. The data were reconstructed to a transverse image series with 5 mm slice thickness using a high frequency image reconstruction algorithm (bone). Window width and level settings were standardised for all measurements (window width, 2000 Hounsfield units; window level, 500 Hounsfield units). Transverse images were reconstructed parallel to the cranial endplate of the vertebral body using multi-planar reconstruction and transferred to a workstation for vertebral volume estimation. The volumes of vertebral bodies were measured using the ImageJ (NIH orgnization, Bethesda, Maryland, USA) and Volumest plugin [17].

Briefly, ImageJ (version 1.47) was downloaded from http://rsbweb.nih.gov/ij/download.html as well as Volumest (http://lepo.it.da.ut.ee/~markkom/volumest/download/) (accession date: 01/04/2013) plug and added to ImageJ software. After opening DICOM images in ImageJ, the scaling of the images is corrected automatically, and volumetric analysis can be continued. On the CT slices the vertebral body was outlined as regions of interest (ROI). To create an ROI, the mouse has to be clicked repeatedly to create line segments. When

finished, one has to click in the small box at the starting point, and ImageJ automatically draws the last segment. After outlining ROI in each slice, the Volumest plug calculates the volume of selected ROI using stereology principles (Figure 1). The volume of each vertebra was measured three times by the same observer (MM).

In order to confirm the accuracy of the ImageJ software, a pilot study was performed in which the sheep lumbar spine was carefully cleaned of surrounding soft tissues using suitable dissection tools. Thereafter, continuous CT transverse images were made as described earlier and imported to ImageJ software for measuring the vertebral body volume of each vertebra. Subsequently, the vertebral bodies were prepared as described previously [15], where the vertebral body pedicles, laminas, and transverse processes were sawed off. The exact vertebral body volume was measured using the Archimedean principle, also known as 'fluid displacement technique' in a measuring cylinder. For this purpose, each vertebral body was immersed in a measuring cylinder filled with distilled water at room temperature. The volumes were measured based on the scale in millimetre increments.

Morphometric comparison

For the morphometric comparison part, a total of four spinal indices and Pavlov's ratio were calculated, based on linear and angular dimensions of the sheep lumbar spine which we published recently (Table 1) [18], and compared to literature on humans (Table 2) [16,19-21]

We compared the absolute values of the vertebral dimensions between sheep and humans. Moreover, to increase the comparison reliability between both species, spinal indices and Pavlov's ratio were also compared. The spinal indices include: Concavity index (CI) defined as the ratio between the dorsal and ventral vertebral body length. The endplate index (EI) was calculated as the ratio between the width and depth of the cranial endplate at the transverse plane. The spinal canal index (SCI) was calculated as the ratio between the width and depth of the spinal canal. The pedicle index (PDI) was defined as the ratio between the width and length of the pedicle. Pavlov's ratio was calculated as the ratio between the depth of both the spinal canal depth and vertebral body [22].

Statistical analysis

In the pilot study, the generated volume values of the vertebral bodies using the fluid displacement technique and ImageJ software were compared using the paired Student's t test. One-way analysis of variance was used to determine the volume differences between the vertebral levels. A P value>0.05 was considered statistically significant.

Intraobservor reliability of vertebral body volume was calculated as the difference between three measurements obtained by the first author. The statistical analysis was performed with Microsoft Excel 2010 package (Microsoft Deutschland GmbH, Unterschleissheim, Germany). The volumes of vertebral bodies and spinal indices were compared between human and sheep vertebrae. The parameter was defined comparable if the ratio sheep/human of each individual vertebra showed variation less than 20%

Results

In the pilot study, the Student's t test revealed that the difference between measured volume values using ImageJ software and fluid displacement technique were not statistically different ($P<0.05$) (Figure 2).

In the present study, the volume intraobserver variability was small with the average difference between three measurements for each vertebra being within 1 cm^3. There were no statistically significant differences in the volume values between the lumbar vertebrae ($P=0.28$). The average volume of each vertebral body increased toward caudal vertebral levels (Table 3). Generally, the volume of the lumbar vertebral bodies was fairly constant at about 16 cm^3. The comparison of the volumes of lumbar vertebral bodies between sheep and humans revealed that sheep had a smaller volume, as much as 48.6% (volume ranging from 34.4% to 54.4%) than humans. Moreover, the comparison revealed that no vertebral level of sheep lumbar spine was comparable to human.

Table 4 lists sheep and human spine indices and Pavlov's ratio. The human lumbar vertebral bodies were wider than they were longer, while the sheep lumbar were longer than they were wider especially at level L5. The human vertebrae were wider and deeper than those of sheep, as much as 17.1 mm (40.6%) and 14.7 mm (45.1%), respectively. In contrast, sheep lumbar vertebrae were longer than human ones, as much as 10.5 mm (28.5%). The concavity index of the sheep was greater than humans especially at the caudal lumbar vertebrae and its values at L1, L2 and L5 were comparable with those of humans. The values of the human EI at all vertebral levels were greater than sheep. The endplate indexes of all of the lumbar vertebral levels were comparable with humans (Table 5).

In both species, the spinal canal was wider than it was deep and increased in width towards the caudal vertebral level. The human spinal canal was wider and deeper than sheep, as much as 10.6 mm (42.7%) and 8.4 mm (45%) respectively. However, the SCI was comparable between both species, except for L1 (Table 5).

The pedicles in both species were higher than they were wide. Sheep pedicles were higher and had a greater lateral angulation than humans, where the latter had a wider and greater

pedicle axis length than sheep. Both findings were most pronounced at the level of the caudal lumbar vertebrae of both species especially at L5. The pedicle index of sheep showed an increasing trend with the ordinal number of lumbar vertebrae. A similar behaviour was observed in humans. The pedicle index values were not comparable at all levels of the lumbar vertebrae (Table 5).

The sheep dorsal spinal process length was smaller than in humans but both of them decreased in a caudal direction. The transverse process length was obviously larger in sheep lumbar vertebrae than in humans and also decreased in a caudal direction. Transverse and dorsal spinous processes have a cranial inclination in sheep.

The human vertebral disc thickness was variable between lumbar vertebral levels. A comparison between the two species revealed that human discs were obviously thicker than sheep. However, the human disc was as much as 69.5% (6.4 mm) thicker than sheep.

The mean Pavlov's ratio value of sheep lumbar vertebrae was 1.7, while the smallest Pavlov's ratio was 1.6 at L5 and the highest was 1.9 at L1. Pavlov's ratio of sheep was greater than in humans. However, Pavlov's ratio of both species was comparable at all vertebral levels (Table 5).

Discussion

The current study aimed to document the normal volume of the sheep lumbar vertebral bodies and to highlight the differences between the sheep and human spine with a view to inform researchers contemplating their use in future studies.

Our results showed that the real volume of the vertebral body, which was measured using fluid displacement technique, agreed well with the volume estimates of ImageJ software. There were no statistical differences detected between them. This indicates that the values of the volume based on ImageJ software are reliable. The interobsarvor variability for each vertebra was less than 1 cm^3. The reason for this difference was most likely due to operator error inherent in making a tracing of the irregular region of interest. Operator error could be affected by spatial resolution and eye-hand coordination, both of them expected to be highly variable among different operators [23]. Therefore, the volume in the present study was measured by the same operator. In order to decrease operator error as much as possible, window width and level were kept similar while estimating the volume.

There is an inverse correlation between slice thickness and accuracy required to perform the volume measurement in the case of increasing slice thickness, thereby reducing the number of CT slices that have to be outlined. In the present study, CT images of the vertebrae were

reconstructed in the transverse plane with 5 mm thickness. A previous study carried out in human spines using a combination of the Cavalieri principle and CT scans showed that both 3- and 5 mm thickness CT scans proved to be sufficiently accurate for measuring volumes [16]. Moreover, the same study reported that the image planes did not affect the accuracy of the volume measurements.

We found that the mean vertebral body volume showed a gradual increase from the cranial towards the caudal vertebral level, but there were no significant differences between the vertebral levels. This finding could be due to the increasing the vertebral body length towards the caudal lumbar vertebrae (Table 1). The comparison of the volumes of vertebral bodies between humans and sheep showed that sheep vertebrae were smaller, as much as 48.6%, than humans. The cause of this difference is most likely to be the upright posture of humans.

In this study, we derived sheep morphometric data from our previous documentation [18]. The comparative data for human parameters were taken from published literature [16,19-21]. Anatomical comparisons have been made between sheep and human spine using manual measurements in cadaveric spines of three- to four-year-old sheep [24]. However, the previous study subjectively compared the spinal dimensions between both species without taking into account the wide scattering effect associated with methodology.

In contrast to a previous study [24], the current study provides an objective comparison using the spinal indices, which were calculated as the ratio between the vertebral dimensions to rule out the heterogeneity of measuring methods and thus making the comparative results more reliable. The spinal indices were defined as being comparable if the ratio sheep/human of each individual vertebral level showed variation less than 20%, because in humans a vertebra is classified as abnormal if an alteration of more than 20% in vertebral dimensions is detected [25]. Noteworthy, the volume of the sheep lumbar vertebral bodies were documented here for the first time.

The comparison between sheep and humans revealed that humans have larger, wider and shorter vertebral bodies and thicker intervertebral discs. These differences can be attributed to the upright posture of the human spine, putting demands relatively larger and shorter caudal vertebral bodies to balance the higher longitudinal loads. This was also probably the explanation for the larger intervertebral disc thickness observed in the human spine, which was up to three times thicker than the sheep disc in the lumbar region [26]. Biomechanically, the highest range of motion around the X and Y axes has been reported at L2-L3 in sheep and L3-L4 in humans [27]. The vertebral morphometry could support this finding, where the current results showed that the vertebral body width and depth decreased from L1 to L2 and then increased until L5, while in humans the vertebral body width and depth decreased from

L1 to L3 and decreased at L4 and L5. In other words, the lumbar spine of both species are composed of two unequal pyramids in coronal plane, which facilitated axial rotation (X axis) and both flexion and extension motion (Y axis) [28].

When comparing pedicle parameters, sheep pedicles are narrower, higher and have greater lateral angulations than humans. Sheep pedicles were not comparable to humans at any lumbar vertebral levels. This means that the pedicle screw designed for humans may not be safely placed in sheep pedicles without modification, the existing screws which are an appropriate length in humans penetrating the ventral vertebral body cortex in sheep. Moreover, the orientation of screw placement should be taken into account to avoid penetrating the lateral cortex of the vertebral body.

The human spinal canal was wider and deeper, and thus covers a greater surface area than in the sheep. We believe this is a kind of adaptation to provide additional support for the upright body weight. The spinal canal area can be evaluated in a variety of ways, such as Pavlov's ratio, which was first proposed as an indicator of the degree of development of the canal narrowing [22]. The spinal canal index and Pavlov's ratio were comparable between humans and sheep.

The spinal processes serve as a lever arm by paraspinal muscles to maintain posture and induce rotation and flexion [29]. In the current study, transverse processes in sheep were longer than in humans. We attribute this to the horizontal position of the sheep spine compared to humans, the sheep paraspinal muscles need a strong support to carry the weight of the abdominal viscera and maintain spinal movements.

One limitation of the present study was the low number of sheep. The number of 5 animals (30 vertebrae) used was the lowest possible to comply with the regulations of 3R but sufficient enough to provide reliable data. Moreover, the animals were of equal age, weight, sex and breed in order to obtain uniformity. However, the repeated sheep dimensions and small variance around the mean indicated that a larger sample was not necessary. Moreover, previous investigators had used similar sample sizes for similar studies [20,24,30].

In conclusion, according to spinal indices results the sheep lumbar spine has good similarity to that of humans in terms of the vertebral endplate regions and spinal canal, suggesting that a sheep spinal model would be appropriate for studying artificial intervertebral discs, implantation of intervertebral fusion, etc. With regard to sheep pedicles, these can be used as a model providing the dimensions of the implant can be adapted to the anatomical dimensions.

References

1. Putz RLV, Müller-Gerbl M. The vertebral column—a phylogenetic failure? A theory explaining the function and vulnerability of the human spine. Clin Anat 1996; 9(3): 205-212.

2. Mann NH, Brown MD, Enger I. Statistical diagnosis of lumbar spine disorders using computerized patient pain drawings. Comput Biol Med 1991; 21(6): 383-397.

3. Ashman R, Bechtold J, Edwards W, Johnston 2nd C, McAfee PC, Tencer A. In vitro spinal arthrodesis implant mechanical testing protocols. J Spinal Disord 1989; 2(4): 274-281.

4. Wall EJ, Bylski-Austrow DI, Shelton FS, Crawford AH, Kolata RJ, Baum DS. Endoscopic discectomy increases thoracic spine flexibility as effectively as open discectomy. A mechanical study in a porcine model. Spine 1998 1; 23(1): 9-15.

5. Reid JE, Meakin JR, Robins SP, Skakle JM, Hukins DW. Sheep lumbar intervertebral discs as models for human discs. Clin Biomech 2002;17(4): 312-314.

6. Gurr KR, McAfee PC, Shih CM. Biomechanical analysis of anterior and posterior instrumentation systems after corpectomy. A calf-spine model. J Bone Joint Surg Am 1988; 70(8): 1182-1191.

7. Ganey T, Libera J, Moos V, Alasevic O, Fritsch KG, Meisel HJ, et al. Disc chondrocyte transplantation in a canine model: a treatment for degenerated or damaged intervertebral disc. Spine 2003 1; 28(23): 2609-2620.

8. Newman E, Turner AS, Wark JD. The potential of sheep for the study of osteopenia: current status and comparison with other animal models. Bone 1995;16(suppl_4): 277S-284S.

9. Nunamaker D. Experimental models of fracture repair. Clin Orthop Relat Res 1998; 355: S56-S65.

10. Bergmann G, Graichen F, Rohlmann A. Hip joint forces in sheep. J Biomech 1999; 32(8): 769-777.

11. Egermann M, Goldhahn J, Schneider E. Animal models for fracture treatment in osteoporosis. Osteoporos Int 2005; 16(suppl_2): 129-138.

12. Turner AS. Experiences with sheep as an animal model for shoulder surgery: strengths and shortcomings. J Shoulder Elbow Surg 2007; 16(5): S158-S163.

13. Ahlgren BD, Lui W, Herkowitz HN, Panjabi MM. Effect of anular repair on the healing strength of the intervertebral disc: a sheep model. Spine 2000; 25(17): 2165-2170.

14. Moore RJ, Osti OL, Vernon-Roberts B, Fraser RD. Changes in endplate vascularity after an outer anulus tear in the sheep. Spine 1976; 17(8): 874-878.

15. Limthongkul W, Karaikovic EE, Savage JW, Markovic A. Volumetric analysis of thoracic and lumbar vertebral bodies. Spine J 2010;10(2):153-158.

16. Odaci E, Sahin B, Sonmez OF, Kaplan S, Bas O, Bilgic S, et al. Rapid estimation of the vertebral body volume: a combination of the Cavalieri principle and computed tomography images. Eur J Radiol 2003; 48(3): 316-326.

17. Merzin M. Applying stereological method in radiology: Volume measurement (Bachelor's thesis), University of Tartu, Tartu, 2008.

18. Mageed M, Berner D, Hohaus C, Jülke H, Brehm W, Gerlach K. Morphometrical dimensions of the sheep thoracolumbar vertebrae as seen on digitised CT images. Lab Anim Res 2013;29(3): 138-147.

19. Abuzayed B, Tutunculer B, Kucukyuruk B, Tuzgen S. Anatomic basis of anterior and posterior instrumentation of the spine: morphometric study. Surg Radiol Anat 2010; 32(1): 75-85.

20. Kumar N, Kukreti S, Ishaque M, Mulholland R. Anatomy of deer spine and its comparison to the human spine. Anat Rec 2000; 260(2): 189-203.

21. Wolf A, Shoham M, Michael S, Moshe R. Morphometric Study of the Human Lumbar Spine for Operation–Workspace Specifications. Spine 2001; 26(22): 2472-2477.

22. Pavlov H, Torg J, Robie B, Jahre C. Cervical spinal stenosis: determination with vertebral body ratio method. Radiology 1987; 164(3): 771-775.

23. Beers GJ, Carter A, Leiter B, Tilak S, Shah R. Interobserver discrepancies in distance measurements from lumbar spine CT scans. Am J Roentgenol 1985; 144(2): 395-398.

24. Wilke HJ, Kettler A, Wenger KH, Claes LE. Anatomy of the sheep spine and its comparison to the human spine. Anat Rec 1997; 247(4): 542-555.

25. Pluijm S, Tromp A, Smit J, Deeg D, Lips P. Consequences of vertebral deformities in older men and women. J Bone Miner Res 2000;15(8):1564-1572.

26. Busscher I, Ploegmakers JJW, Verkerke GJ, Veldhuizen AG. Comparative anatomical dimensions of the complete human and porcine spine. Eur Spine J 2010;19(7): 1104-1114.

27. Wilke HJ, Kettler A, Claes LE. Are sheep spines a valid biomechanical model for human spines? Spine 1997; 22(20): 2365-2374.

28. Masharawi Y, Salame K, Mirovsky Y, Peleg S, Dar G, Steinberg N, et al. Vertebral body shape variation in the thoracic and lumbar spine: characterization of its asymmetry and wedging. Clin Anat 2007; 21(1): 46-54.

29. Haussler KK. Anatomy of the thoracolumbar vertebral region. Vet Clin North Am Equine Pract 1999;15(1): 13-26.

30. Wilke HJ, Kettler A, Claes LE. Are sheep spines a valid biomechanical model for human spines? Spine 1997 15; 22(20): 2365-2374.

Table 1 Mean and standard deviation of measured sheep lumbar vertebrae dimensions (mm, °degrees)

	VBW	VBD	VBLd	VBLv	PDW	PDH	PAA°	PAL	TPL	SPL	DT	SCW	SCD
L1	24.5 ± 2.2	18.3 ± 0.8	36.2 ± 0.8	34.2 ± 0.5	6.0 ± 1.0	23.9 ± 3.3	22.4 ± 1.3	33.6 ± 4.0	94.2 ± 9.2	26.3 ± 0.4	3.3 ± 1.0	9.8 ± 0.6	9.8 ± 0.7
L2	23.7 ± 3.6	17.7 ± 1.1	37.6 ± 0.8	35.3 ± 1.1	7.3 ± 0.6	27.9 ± 1.3	24.7 ± 0.8	36.1 ± 1.5	116.4 ± 10.3	26.8 ± 0.4	2.6 ± 0.5	14.4 ± 0.4	10.4 ± 1.1
L3	24.4 ± 2.7	18.0 ± 1.9	38.4 ± 1.0	36.2 ± 0.5	7.7 ± 1.6	28.8 ± 1.3	25.7 ± 1.5	37.1 ±1.1	123.4 ± 11.7	26.8 ± 0.4	2.6 ± 0.5	15.2 ± 1.1	10.0 ± 1.2
L4	24.0 ± 3.1	17.9 ± 2.2	39.2 ± 0.9	37.4 ± 0.6	8.2 ± 0.7	27.5 ± 1.4	26.5 ± 1.2	36.7 ± 1.9	128.6 ± 10.6	26.2 ± 0.3	2.7 ± 0.5	15.2 ± 3.3	10.2 ± 1.0
L5	24.7 ± 2.6	17.1 ± 2.1	39.9 ± 1.9	38.9 ± 0.3	8.4 ± 0.5	29.0 ± 1.5	27.5 ± 0.8	36.5 ± 1.2	130.9 ± 10.6	25.6 ± 0.4	2.9 ± 0.5	16.9 ± 1.2	10.7 ± 1.0
L6	32.0 ± 7.3	16.3 ± 1.7	40.7 ± 1.0	38.7 ± 2.9	8.3 ± 1.6	27.2 ± 1.9	32.0 ± 1.7	35.2 ± 2.8	127.3 ± 7.8	25.53 ± 0.3	2.9 ± 0.3	18.9 ± 1.6	12.2 ± 0.7

VBW; vertebral body width, WBD; vertebral body depth, VBLd; vertebral body length dorsal, VBLv; vertebral body length ventral, DT; disc thickness. SCW; spinal canal width, SCD; spinal canal depth, SPL; spinal process length, TPL; transverses process length, PDW; pedicle width, PDH; pedicle length, PAL; pedicle axis length, PAA; pedicle axis angle.

Table 2 Mean and standard deviation of measured human lumbar vertebrae dimensions (mm, °degrees) from literature on humans [19-21]

	VBW	VBD	VBLd	VBLv	PDW	PDH	PAA°	PAL	TPL	SPL	DT	SCW	SCD
L1	40.9 ± 3.8	31.0 ± 3.0	27.0 ± 2.1	26.7 ± 1.5	5.6 ± 1.3	15.1 ± 1.8	11.8 ± 1.3	44.8 ± 2.8	81.8 ± 5.1	30.0 ± 3.7	7.9 ± 1.8	23.7 ± 0.9	19.0 ± 0.7
L2	39.8 ± 4.6	32.5 ± 2.3	27.4 ± 2.1	27.0 ± 2.7	7.7 ± 1.5	14.8 ± 1.6	11.0 ±1.7	46.9 ± 3.6	80.4 ± 4.6	31.5 ± 4.6	10.0 ± 1.6	23.8 ± 0.7	18.2 ± 0.5
L3	34.1 ± 3.8	31.2 ± 4.0	27.3 ± 2.9	27.5 ± 2.6	8.9 ± 1.9	14.5 ± 1.9	12.8 ± 2.2	47.6 ± 3.7	89.4 ± 5.5	33.5 ± 5.7	9.9 ± 1.8	24.3 ± 0.6	17.5 ± 0.5
L4	44.1 ± 4.6	33.0 ± 2.8	26.0 ± 1.7	26.2 ± 2.2	11.4 ± 1.8	14.8 ± 2.1	14.1 ± 2.1	47.6 ± 4.4	90.5 ± 5.7	32.8 ± 5.3	9.7 ± 2.3	25.4 ± 0.5	18.6 ± 0.7
L5	48.1 ± 3.8	34.9 ± 4.1	22.9 ± 1.7	28.5 ± 2.5	13.7 ± 2.2	15.6 ± 2.3	18.5 ± 3.9	46.6 ± 5.3	93.7 ± 5.9	26.0 ± 5.7	8.2 ± 2.3	27.1 ± 0.9	19.7 ± 0.5

VBW; vertebral body width, WBD; vertebral body depth, VBLd; vertebral body length dorsal, VBLv; vertebral body length ventral, DT; disc thickness. SCW; spinal canal width, SCD; spinal canal depth, SPL; spinal process length, TPL; transverses process length, PDW; pedicle width, PDH; pedicle length, PAL; pedicle axis length, PAA; pedicle axis angle.

Table 3 Mean and standard deviation of sheep and human lumbar vertebral body volume (cm^3)

	Human*	Sheep
L1	25.6 ± 2.0	13.9 ± 1.2
L2	30.9 ± 0.4	14.3 ± 1.7
L3	33.8 ± 1.4	14.7 ± 2.9
L4	34.2 ± 1.0	16.9 ± 3.5
L5	35.8 ± 2.1	17.6 ± 2.9
L6	-	18.2 ± 3.1

The sheep vertebral body volume was measured using ImageJ software. * Human data were taken from Odaci *et al*. [16].

Table 4 Spine indices of sheep and human lumbar vertebrae

	CI	EI	SCI	PDI	Pavlov's ratio
Sheep					
L1	105.8	74.7	100.0	25.1	1.9
L2	106.5	74.7	72.2	26.2	1.7
L3	106.1	73.8	65.8	26.7	1.8
L4	104.8	74.6	67.1	29.8	1.8
L5	102.6	69.2	63.3	29.0	1.6
L6	105.2	50.9	154.9	30.5	1.3
Human					
L1	101.1	75.8	80.2	37.1	1.6
L2	101.5	81.7	76.5	52.0	1.8
L3	99.3	91.5	72.0	61.4	1.8
L4	99.2	74.8	73.2	77.0	1.8
L5	80.4	72.6	72.7	87.8	1.8

CI (concavity index was calculated as ratio between the dorsal and ventral vertebral body length), EI (Endplate index was calculated as ratio between the width and depth of cranial endplate at the transverse plane), SCI (spinal canal index was calculated as ratio between the width and depth of spinal canal), PDI (pedicle index was defined as the ratio between the width and length of the pedicle. The Pavlov's ratio was calculated as the ratio between the depth of both spinal canal depth and vertebral body.

Table 5 Comparison of the absolute values of each dimension between humans and sheep

	Concavity index	Endplate index	Spinal canal index	Pedicle index	Pavlov's ratio	Vertebral body volume
L1	C	C	NC	NC	C	NC
L2	C	C	C	NC	C	NC
L3	NC	C	C	NC	C	NC
L4	NC	C	C	NC	C	NC
L5	C	C	C	NC	C	NC

The ratio between human and sheep values of a dimension was calculated for each vertebral level. If the variance of these ratios was less than 20% between the same vertebral level of both species that particular dimension was defined as 'comparable'. C - comparable, NC - not comparable.

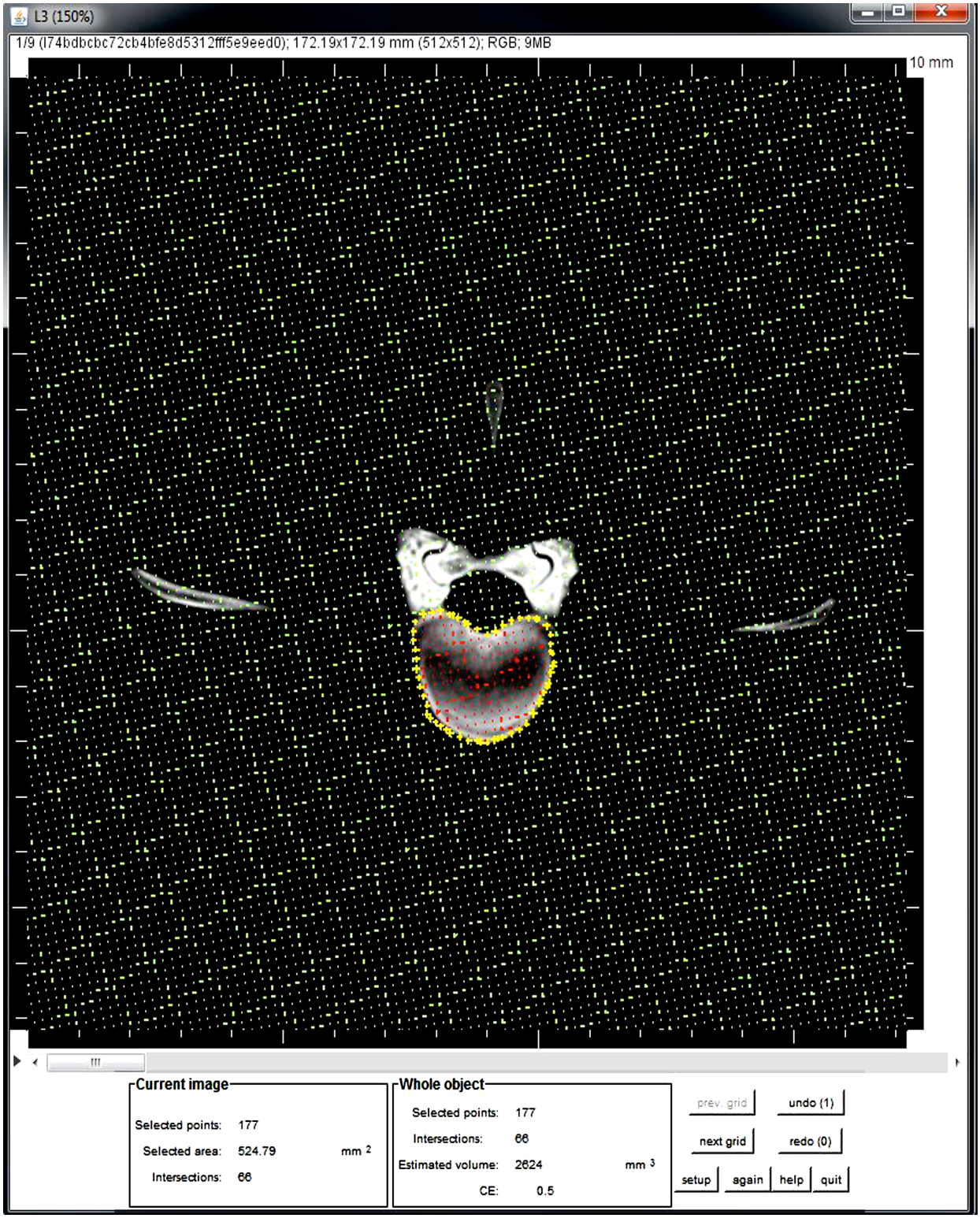

Figure 1. Estimation the vertebral body volume using ImageJ. The vertebral body was outlined (yellow stars), subsequently the Volumest plugin calculates automatically the volume from the area (red stars) and the slice thickness of each image. Finally, these values per image were added up to calculate the volume.

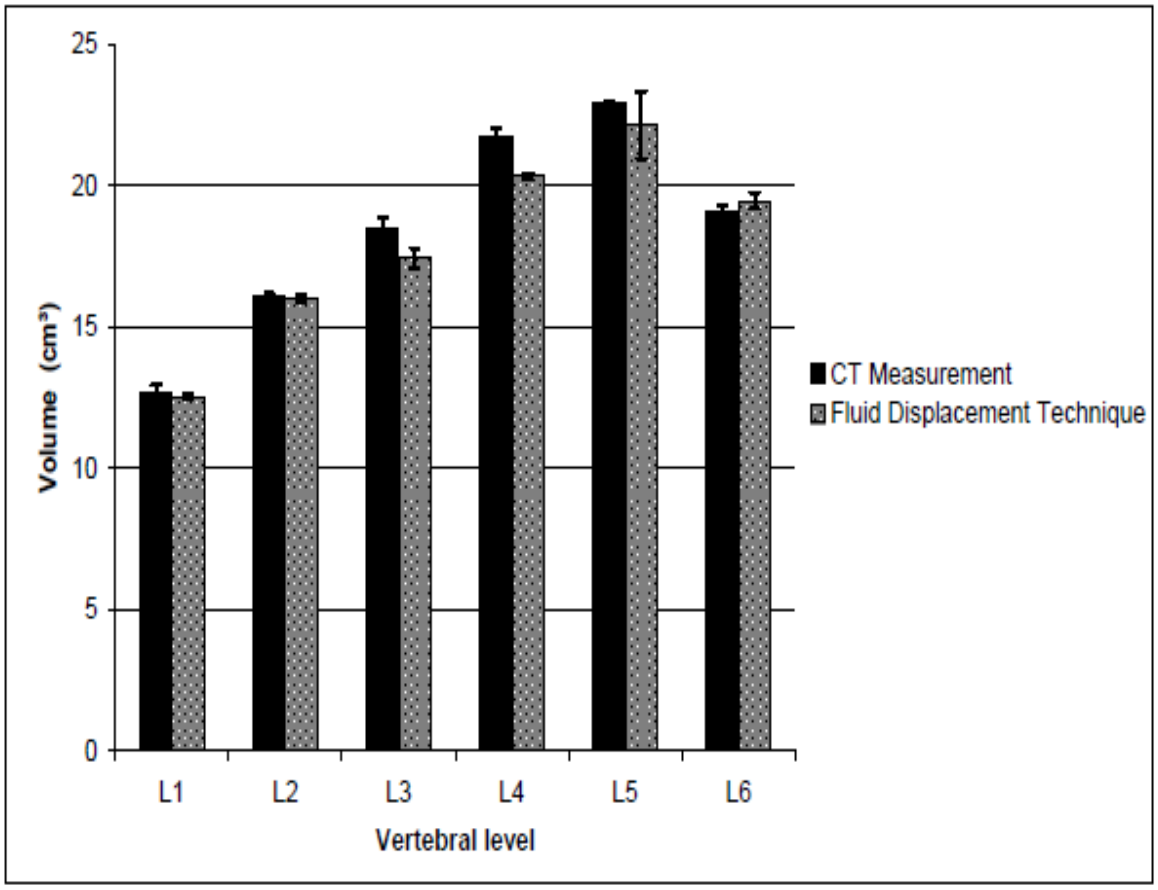

Figure 2. The means of the vertebral body volumes (cm³) of the sheep using imageJ software compared to real volume of the same vertebrae, which was measured using fluid displacement technique.

3.3 Publication 3: Morphometrical analysis of the thoracolumbar dural sac in sheep using computed assisted myelography

Mahmoud Mageed[1, 2]*, Jean-Claude Ionita[1], Eberhard Ludewig[3], Walter Brehm[1] and Kerstin Gerlach[1]

Veterinary and Comparative Orthopaedics and Traumatology 2014;27(2):124-129.

http://dx.doi.org/10.3415/VCOT-13-09-0116
PMID: 24493357

[1]Large Animal Clinic for Surgery, Faculty of Veterinary Medicine, University of Leipzig, An den Tierkliniken 21, 04103, Leipzig, Germany.

[2]Department of Surgery and Anaesthesia, Faculty of Veterinary Medicine, University of Khartoum, Shambat, PO Box 32, Khartoum, Sudan.

[3]Department of Small Animal Medicine, Faculty of Veterinary Medicine, University of Leipzig, An den Tierkliniken 23, 04103, Leipzig, Germany.

* Correspondence to: Mahmoud Mageed

Large Animal Clinic for Surgery, Faculty of Veterinary Medicine, University of Leipzig, An den Tierkliniken 21, 04103 Leipzig, Germany.

Phone: +49 341 9738264

Fax: +49 341 9738218

E-mail: mahmoud.mageed@hotmail.com

Received: September 24, 2013

Accepted: November 17, 2013

Pre-published online: February 4, 2014

Keywords

Animal model, ovine, dural sac, myelography, computed tomography

Summary

Objectives: Sheep are frequently used as animal models in experimental spinal injury studies. Therefore, extensive knowledge of ovine spinal dimensions is essential for experimental design and interpretation of results obtained in these trials. This study aimed to obtain quantitative morphometrical data of the thoracolumbar dural sac in sheep and determine the anatomical relationship between the dural sac and the vertebral canal.

Methods: Computed assisted myelography scanning was carried out in five adult German Black-Headed Mutton sheep under general anaesthesia. Transverse images were acquired with 2 mm slice thickness from T1 to L6. Sagittal and transverse diameters and the cross-sectional area of the dural sac and vertebral canal were measured. To determine the anatomical relationship between the dural sac and vertebral canal, PDSD (pedicle-dural sac distance), epidural space as well as SAC (available space for the dural sac) were calculated.
Results: Sagittal diameters of the dural sac ranging from 5.1 to 12.0 mm. Transverse diameters ranged from 5.6 to 12.2 mm. The dural sac area covered 45.9% and 49.0% of the thoracic and lumbar vertebral canal area. The PDSD in the lumbar vertebrae was up to 15.8% larger than in the thoracic ones. The dural sac area was significantly positive correlated with the transverse diameter and area of the vertebral canal.

Clinical significance: The lumbar vertebral canal shows more space for the dural sac, which seems to be safer for testing new spinal implants.

Introduction

New spinal implants and surgical procedures have been well developed and modified for surgical treatment of spinal instability as well as spinal cord injuries and therefore they should be tested before being accepted into clinical use (1). Animal models are most commonly used for such tests, where they are available and provide more homogeneity when selected for age, breed, and sex than human specimen did (2). Non-human primates provide an excellent model thanks to their analogy with humans, but are not cost-efficient, require stringent controls, vectors of severe zoonotic diseases, and cause ethical pressures (3,4). Cats, dogs and rats have also been used as animal models for research in spine and spinal cord trauma (5-8), but sheep are especially well accepted as an ethical animal model as they have a similar body weight to humans, and are sufficiently large to allow serial sampling and multiple experimental procedures (9,10). Furthermore, sheep have been reported as a suitable model for human spinal research, due to similarity of the bony and vascular anatomy of both species (11).

In humans the shape of the vertebral canal after injury, as determined by the sagittal-to-transverse diameter ratio, was predictive of neurological deficit, where the ratio of sagittal-to-transverse diameter at the level of injured spinal cord was significantly smaller in patients with a neurological deficit than in those without one (12). The vertebral canal area can be evaluated in different ways. The ratio of the sagittal diameter of the cervical canal to that of the vertebral body was first proposed as an indicator of the degree of developmental canal narrowing (13). With the development of diagnostic methods, other reliable means for assessing vertebral canal area were introduced, such as the measurement of the ratio between spinal canal area and vertebral body obtained from computed tomography (CT) scans or computed assisted myelography (CAM). CAM has been found to be more sensitive than myelography for characterising morphology of the spine in humans, horses, and dogs (14-18). The technique is considered to be particularly helpful for diagnosing spinal cord atrophy, spinal stenosis, and vertebral malformation/malarticulation (16, 19-23). Cross-sectional area measurements from CT images are a sensitive method for quantifying spinal components (24-27). The use of area ratios has been found to be a good means to help correct for differences in body sizes (26).

Despite the increasing use of the sheep as animal model for human spinal research, no morphometrical computed tomographical studies related to the dural sac of the thoracolumbar spine in normal sheep were found at the time of this study. Therefore, the current study aimed to obtain quantitative morphometrical data of the thoracolumbar dural sac in sheep, and determine the anatomical relationship between the dural sac and surrounding osseous structures of the vertebral canal.

Material and Methods

Animals

For the present study, five healthy female German Black-Headed Mutton sheep without history or clinical signs related to spinal diseases were included. The mean age of the sheep was 2.0 ± 0.4 years. The mean body weight was 80.6 ± 28.7 kg. This study was approved by the Animal Welfare Commission, Regional Office Leipzig (Landesdirektion Sachsen TVV-No. 14/03).

Anaesthesia

Each sheep was fasted for 24 hours and deprived of water for 12 hours before being premedicated with 0.1 mg/kg atropine sulphate[1], and a combination of 0.1 mg/kg butorphanol tartrate[2] and 0.2 mg/kg midazolam[3] administered intravenously. Anaesthesia was induced with 3 mg/kg ketamine chlorhydrate[4] intravenously. After endotracheal intubation, anaesthesia was maintained with isoflurane[5] delivered in oxygen through an endotracheal tube.

Myelography technique

After induction of general anaesthesia, the sheep were positioned in lateral recumbency on a radiographic table. The lumbar tap site was clipped and aseptically prepared. The most dorsocranial edge of the spinous process of L6 was identified. Thereafter, a 3.5 inch, 22-G spinal needle[6] was introduced through the skin on the midline at 90° on the midsagittal axis of the vertebral body with the bevel directed cranially. The needle was then slowly advanced until contact was made with the ventral floor of the vertebral canal and then retracted 2 mm before the stylet was removed to check the passive cerebrospinal fluid drip (CSF). To facilitate CSF dripping through the needle hub, the jugular veins were compressed. 1 to 2 ml of CSF fluid was aspirated before injecting the contrast solution through a flexible extension tube connecting the needle and syringe. A dose of 0.45 ml/kg of non-ionic iodinate contrast media[7] was injected slowly (about 2-3 minutes). The sheep were positioned at different positions to facilitate contrast media distribution in the subarachnoidal space then positioned

[1] Atropinum sulfuricum 0.5 mg Eifelango®, Eifelango, Bad Neuenahr-Ahrweiler, Germany

[2] Alvegesic®, CP-Pharma GmbH, Burgdorf, Germany

[3] Midazolam, B. Braun; B.Braun, Melsung, Germany

[4] Ursotamin®, Serumwerk Bernburg AG, Bernburg, Germany

[5] Isofluran CP®, CP-Pharma GmbH, Burgdorf, Germany

[6] BD spinal needle, BD, Madrid, Spain

[7] Solutrast® 200M, Bracco Imaging Deutschland GmbH, Konstanz, Germany

on the CT scanner table for scanning. After scanning the sheep were kept under clinical observation for 72 hours.

CT examination

The sheep were positioned in dorsal recumbency with the hind limbs flexed to minimise curvatures of the thoracolumbar spine and positioning aids tools were used to obtain a perpendicular position of the spine relative to the x-ray beam of the gantry. Contiguous slices were obtained from the cranial aspect of T1 to the caudal aspect of L6 with a multi-detector-row helical CT unit[8]. Technical settings were 140 kV, 255 mAs, 0.75 second tube rotation and a pitch of 0.533. The data were reconstructed to transverse image series with 2 mm slice thickness using a high-frequency image reconstruction algorithm (bone). Multi-planar reformatting software was used as needed to reformat the transverse slices parallel to the cranial endplate of the vertebral body. CT images were transferred to a workstation and reviewed with picture archiving and communication software[9], which allows quantitative measuring of the distance and the area on CT images in DICOM format. From the transverse images series, a single CT image through the middle third of the vertebral body was selected for measuring. This level demonstrates individual features of each vertebra relative to the adjacent vertebra. Moreover, at this level the lamina and pedicles are completely surrounding the dural sac. For all measurements, images were displayed using a 2500 window width and 480 window level on the same workstation.

The parameters of the dural sac and vertebral canal included sagittal and transverse diameters and cross-sectional area (Figure 1). In order to depict the anatomical relation between the dural sac and surrounding osseous structures the pedicle–dural sac distance (PDSD), epidural space areas and available space for dural sac (SAC) were calculated. The PDSD was defined as the distance between the axial border of the right/left pedicle and the lateral limit of the dural sac, which was delineated with contrast solution. The PDSD was calculated by subtracting the distance between the ipsilateral border of the dural sac and axial border of the contralateral pedicle from the transverse diameter of the vertebral canal. Epidural space area was calculated by subtracting the dural sac area from vertebral canal area. The SAC is determined by subtracting the sagittal diameter of the dural sac from the sagittal diameter of the vertebral canal. All measurements were performed by the same operator (MM). Each parameter was measured three times and then six times in one sheep, to evaluate for the intraobserver error. There was at least a 3day interval between the measurements of each parameter.

[8] Philips Brilliance 6 CT Scanner, Hamburg, Germany

[9] CuraSmartClient, curasystems GmbH, Ettlingen, Germany

Statistical analysis

Intraobserver reliability was calculated as the difference between three measurements obtained by the same operator. One-way analysis of variance and the Scheffe test were used to determine the differences between the values of the same parameter at the vertebral levels. The association between the different measurements was assessed using Pearson's correlations. The level of significance was set at $P < 0.001$ and $r > 0.7$. All statistical tests were performed using SPSS software version 20 for Windows[10].

Results

Our analysis showed no statistical difference between measuring three and six times. Therefore, we chose to measure each parameter only three times. All sheep recovered well from the anaesthesia during the first 25 minutes after being disconnected from the anaesthetic machine. Four sheep were able to stand on all four limbs without assistance within one hour after the CT scan, whereas the fifth sheep stood after 6 hours and showed a mild lameness during the first 24 hours. It therefore received a single dose (0.5mg/kg, IV) of meloxicam[11] and recovered well.

For morphometrical analysis, each parameter was measured three times to minimise the intraobserver error, which made a total of 1995 readings for all parameters. Intraobserver variability was small as the average difference between three measurements for each vertebra was within 1 mm and 1mm² for cross-sectional area.

Detailed measurements of the sheep thoracolumbar dural sac and vertebral canal are shown in Table 1. The sagittal diameters of the dural sac for the T1 to L6 ranged from 5.1 mm to 12.0 mm (mean = 7.6 mm). The maximum mean sagittal diameter of the dural sac was observed at the level of T1 vertebra (9.4 ± 1.6 mm) and the lowest was observed at T5 (6.0 ± 1.5 mm). For the transverse diameter, the values varied between 5.6 mm and 12.2 mm (mean = 7.6 mm). The minimum transverse diameter was seen at the T5 vertebral level (6.0 ± 1.5 mm) and the maximum at the T1 vertebral level (11.3 ± 0.7 mm). The mean cross-sectional area for the dural sac was 45.5 mm² in the thoracic spine. This represented approximately 45.9% of the thoracic vertebral canal transverse area (mean = 107.2 mm²). In the lumbar region the mean transverse area for the dural sac was 51.6 mm², which represented 49.0% of the vertebral canal area (mean = 117.1 mm²). Significant differences ($P < 0.001$) were detected for each dimension of the dural sac between the vertebral levels (Table 1).

[10] SPSS, Inc., Chicago, IL, USA

[11] Metacam®, Boehringer Ingelheim, Ingelheim am Rhein, Germany

The maximum mean sagittal diameter of the vertebral canal over the entire thoracolumbar spine was found at T1 (15.4 ± 1.5 mm) and the minimum at T5 (8.8 ± 2.3 mm). The maximum transverse diameter was observed at T1 (23.3 ± 3.0 mm). The minimum transverse diameter was found at T9 (10.8 ± 0.8 mm). The mean vertebral canal area was 107.2 and 117.1 mm² in the thoracic and lumbar region, respectively. Significant differences ($P < 0.001$) were observed within each parameter of the vertebral canal between the vertebral levels (Table 1).

There was no statistically significant difference observed between the right and left PDSD. However, the dural sac tended to extend more to the left. The maximum mean PDSD was observed at the level of the T1 vertebra (4.4 ± 1.3 mm) and the lowest was observed at T6 (0.9 ± 0.2 mm). In the lumbar spine the PDSD was 15.8% larger than in the thoracic vertebrae (Table 1).

In the thoracic region, the SAC ranged from 2.2 to 6.0 mm (mean = 3.3 mm) and were greatest at T1 (6.0 ± 1.2 mm) and lowest at T10 (2.4 ± 1.6 mm), whereas in the lumbar region, SAC values ranged from 3.0 to 4.1 mm (mean = 3.3 mm) and were greatest at L6 (4.1 ± 0.8 mm) and lowest at L3 (3.0 ± 0.9 mm) (Table 1).

When vertebral levels were analysed individually, no significant correlations were found between dimensions of the dural sac and dimensions of vertebral components. When all segments (T1-L6) were analysed as a group, area measurements of the dural sac were significantly correlated ($r > 0.7$; $P < 0.001$) with the vertebral canal area. Significant positive correlations were also identified between the following dimensions: The area of the dural sac and both area and transverse diameter of the vertebral canal; the area of the vertebral canal and PDSD, epidural space area and both sagittal and transverse diameters of vertebral canal (Table 2).

Discussion

The current study aimed to obtain quantitative morphometrical data of the thoracolumbar dural sac in normal sheep using computed assisted myelography, and to determine the anatomical relationship between the dural sac and surrounding osseous structures of the vertebral canal.

The dural sac area covered 45.9% and 49.0% of the thoracic and lumbar vertebral canal transverse area and was significantly positive correlated with the transverse diameter and area of the vertebral canal. The PDSD in the lumbar vertebrae was up to 15.8% larger than in the thoracic ones.

The dural sac did not appear uniform in diameter owing to the normal widening of the dural sac in the most cranial thoracic and lumbar dural sac as a result of the brachial and lumbosacral spinal intumescences, respectively. The variability of the transverse diameter of the dural sac with its cross-sectional area was more prominent than that of the sagittal diameter. This indicates the transverse diameter is a more significant measurement for the cross-sectional area, and the most cranial thoracic and lumbar enlargements are more dependent on the transverse diameter than on the sagittal diameter. This finding was supported by Sherman et al. (28), who reported that cervical enlargement is usually not visualised on sagittal images because it is mainly present in the axial plane. Nonetheless, it may be seen on coronal images.

Transverse diameters of the vertebral canal were greater than sagittal diameters in all thoracolumbar vertebral levels. In CT images, the epidural space was visible only in the lateral portions of the canal in most thoracolumbar vertebral levels, particularly at the mid and caudal thoracic spine. Epidural space areas were calculated by subtracting the dural sac area from the vertebral canal area. Mean epidural space areas represented approximately 54.1% of the vertebral canal area for the thoracic spine and 51.0% for the lumbar spine.

In the current study, an attempt was made to define the anatomical relationships of the thoracolumbar osseous structures to the dural sac, which represented an important factor for spinal implants and surgical procedures planning. We measured the little space between the dural sac and pedicles at all thoracolumbar vertebral levels. The results showed that the PDSD of lumbar vertebrae was up to 15.8% larger than that of thoracic vertebrae, meaning that the lumbar pedicles are safer for application of spinal implants, such as intrapedicular screw, than the thoracic region. Furthermore, our data showed that PDSD space was smaller in the lumbar region (ranged from 1.6 mm to 2.9 mm) and that there were no significant differences among lumbar levels from L1 to L5. However at the L6 level, the space between the dural sac and pedicle was much wider, which means a spinal implant is safer to be tested at L6 than other lumbar levels.

The SAC is recommended to be an effective indicator of spinal stenosis in human patients (29). The minimum SAC values in the lumbar region were greater than the SAC values of all of the thoracic vertebrae except T1. The clinical relevance of this finding is that the lumbar spine is safer than the thoracic region for application of spinal implants.

The myelogram protocol in this study was modified from the protocol used for the large dogs (30). The post meylography complications were observed in one sheep as a delay in standing without assistance and mild lameness in the first 24 hours. This sheep needed 6 attempts before the needle was able to be positioned in the subarachnoid space. The main

reason for repeating puncture was the thick layer of subcutaneous adipose tissue (weight= 115 kg), which reduced the exact palpation of the landmarks, thus increasing the likelihood of causing more damage to the neural structures with each attempt.

The accuracy of the morphometrical study may be affected by several factors such as positioning, scanning settings (31), imaging parameters and post-processing, in particular the reconstruction algorithm and the reformatting parameters, as well as the mode of display (32).

Dorsal recumbency is the position of choice for spine CT imaging, because it ensures minimal respiratory movements of the spine and minimised curvatures of the spine. Therefore, the sheep were positioned in dorsal recumbency perpendicular to the x-ray beam. It is crucial to position the spine perpendicular to the x-ray beam of the gantry, because the diameter and area dimensions of objects located in the transverse plane can be altered if they are not perpendicular to the scan plane (33). Decreasing slice thickness (2 mm in this study) reduces the amount of volume averaging artefact and thus improves spatial resolution but increases the image noise. To keep the noise at an acceptable level, high mAs and wide window display should be used (34, 35). In the present study, the CT scanning setting was 255 mAs and 2500 Hounsfield units window width. The scanning parameters of this study are consistent with published spinal CT imaging protocol (35). Operator factors can also influence the measurements accuracy. In order to minimise operator factors, all measurements for this database were performed by a single observer (MM) (36). In a morphometric study of the canine lumbosacral spine, Jones et al. (26) determined that the accuracy of transverse area measurements was lower than diameter measurements. This was considered to be most likely due to operator error related to irregular hand tracing of the regions of interest.

One limitation of this study was the small sample size. The number of 5 animals used was the lowest possible to comply with the rules of 3Rs (*Replacement*; use of non-animal methods, *Reduction*; reduce the number of animals used and *Refinement*; improve animal welfare), but sufficient enough to provide reliable data (37). Furthermore, to overcome the problem of small sample size, significance for the correlation analysis was set using a high r value (> 0.7) and a low P value (< 0.001).

In conclusion, this study provides a comprehensive quantitative morphometrical database for the sheep thoracolumbar dural sac and its relation to osseous structures of the vertebral canal. Findings from this study indicate that the lumbar vertebral canal has greater space for the dural sac than the thoracic vertebrae. Based on this finding we recommend using lumbar

vertebrae for pre-clinical testing of spinal implants, such as intrapedicular screw, to avoid neural structure injuries, when sheep are used as an animal model.

Acknowledgments

The authors would like to thank Mrs. Franziska Benesch for providing the experimental animals, Mrs. Ines Merseburger for her assistance in CT scanning, Mr. Andreas Malter for his help in preparing the figures of this study and the department of Small Animal Medicine of the Faculty of Veterinary Medicine of the University of Leipzig for providing the equipment and facilities for the study.

Conflict of interest

The authors declare that there is no conflict of interest.

References

1. Wilke H, Wenger K, Claes L. Testing criteria for spinal implants: recommendations for the standardization of in vitro stability testing of spinal implants. Eur Spine J 1998; 7: 148–154.
2. Dickey P, Dumas A, Bednar A. Comparison of porcine and human lumbar spine flexion mechanics.Vet Comp Orthop Traumatol 2003; 16: 44-49.
3. Nout YS, Rosenzweig ES, Brock JH, Strand SC, Moseanko R, Hawbecker S, et al. Animal models of neurologic disorders: a nonhuman primate model of spinal cord injury. Neurotherapeutics 2012; 9: 380-392.
4. Martini L, Fini M, Giavaresi G, Giardino R. Sheep model in orthopedic research: a literature review. Comp Med 2001; 51: 292-299.
5. Rossignol S, Chau C, Giroux N, Brustein E, Bouyer L, Marcoux J, et al. The cat model of spinal injury. Prog Brain Res 2002; 137: 151-168.
6. Frigon A. The Cat Model of Spinal Cord Injury. In: Aldskogius H, editor. Animal Models of Spinal Cord Repair. New York: Humana Press; 2013. pg. 159-183.
7. Soubeyrand M, Laemmel E, Dubory A, Vicaut E, Duranteau J. Rat model of spinal cord injury preserving dura mater integrity and allowing measurements of cerebrospinal fluid pressure and spinal cord blood flow. Eur spine j 2013: 1-10.
8. Konrad P, Tacker W, Levy W, Reedy D, Cook J, Geddes L. Motor evoked potentials in the dog: effects of global ischemia on spinal cord and peripheral nerve signals. Neurosurgery 1987; 20: 117-124.
9. Benneker M, Gisep A, KrebsL, Boger A, Heini P, Boner V. Development of an in vivo experimental model for percutaneous vertebroplasty in sheep. Vet Comp Orthop Traumatol 2012; 25: 173–177.

10. Turner AS. Experiences with sheep as an animal model for shoulder surgery: strengths and shortcomings. J Shoulder Elbow Surg 2007; 16: S158-S163.
11. Cain CC, Fraser RD. Bony and vascular anatomy of the normal cervical spine in the sheep. Spine 1995; 20: 759-764.
12. Vaccaro AR, Nachwalter RS, Klein GR, Sewards JM, Albert TJ, Garfin SR. The significance of thoracolumbar spinal canal size in spinal cord injury patients. Spine 2001; 26: 371-376.
13. Pavlov H, Torg J, Robie B, Jahre C. Cervical spinal stenosis: determination with vertebral body ratio method. Radiology 1987; 164: 771-775.
14. Arlien-Søborg P, Kjaer L, Praestholm J. Myelography, CT, and MRI of the spinal canal in patients with myelopathy: a prospective study. Acta Neurol Scand 1993; 87: 95-102.
15. Azar-Kia B, Fine M, Naheedy MH. Importance of metrizamide CT for evaluation of the thoracic spine. Comput Radiol 1985; 9: 233-241.
16. Badami JP, Norman D, Barbaro NM, Cann CE, Weinstein P, Sobel D. Metrizamide CT myelography in cervical myelopathy and radiculopathy: correlation with conventional myelography and surgical findings. Am J Roentgenol 1985; 144: 675-680.
17. Nout Y, Reed S. Cervical vertebral stenotic myelopathy. Equine Vet Educ 2003; 15: 212-223.
18. Sharp NJ, Cofone M, Robertson ID, DeCarlo A, Smith GK, Thrall DE. Computed tomography in the evaluation of caudal cervical spondylomyelopathy of the Doberman Pinscher. Vet Radiol Ultrasound 1995; 36: 100-108.
19. da Costa RC, Echandi RL, Beauchamp D. Computed tomography myelographic findings in dogs with cervical spondylomyelopathy. Vet Radiol Ultrasound 2012; 53: 64-70.
20. Hara Y, Tagawa M, Ejima H, Orima H, Fujita M. Usefulness of computed tomography after myelography for surgery on dogs with cervical intervertebral disc protrusion. J Vet Med Sci 1994; 56: 791-794.
21. Hirabuki N, Mitomo M, Miura T, Hashimoto T, Kawai R, Kozuka T. Computed tomographic myelography characteristics of spinal cord atrophy in juvenile muscular atrophy of the upper extremity. Eur J Radiol 1991; 13: 215-219.
22. Naganawa T, Miyamoto K, Ogura H, Suzuki N, Shimizu K. Comparison of magnetic resonance imaging and computed tomogram-myelography for evaluation of cross sections of cervical spinal morphology. Spine 2011; 36: 50-56.
23. Ogura H, Miyamoto K, Fukuta S, Naganawa T, Shimizu K. Comparison of magnetic resonance imaging and computed tomography-myelography for quantitative evaluation of lumbar intracanalar cross-section. Yonsei Med J 2011; 52: 137-144.

24. Bolender N, Schönström N, Spengler D. Role of computed tomography and myelography in the diagnosis of central spinal stenosis. J Bone Joint Surg Am 1985; 67: 240-246.

25. Inoue H, Ohmori K, Takatsu T, Teramoto T, Ishida Y, Suzuki K. Morphological analysis of the cervical spinal canal, dural tube and spinal cord in normal individuals using CT myelography. Neuroradiology 1996; 38: 148-151.

26. Jones J, Wright J, Bartels J. Computed tomographic morphometry of the lumbosacral spine of dogs. Am J Vet Res 1995; 56: 1125-1132.

27. Yu Y, Du Boulay G, Stevens J, Kendall B. Computed tomography in cervical spondylotic myelopathy and radiculopathy: visualisation of structures, myelographic comparison, cord measurements and clinical utility. Neuroradiology 1986; 28: 221-236.

28. Sherman J, Nassaux P, Citrin C. Measurements of the normal cervical spinal cord on MR imaging. Am J Neuroradiol 1990; 11: 369-372.

29. Tierney RT, Maldjian C, Mattacola CG, Straub SJ, Sitler MR. Cervical spine stenosis measures in normal subjects. J Athl Train 2002; 37: 190-193.

30. Roberts R, Selcer B. Myelography and epidurography. Vet Clin North Am Small Anim Pract 1993; 23: 307-329.

31. Way TW, Chan H-P, Goodsitt MM, Sahiner B, Hadjiiski LM, Zhou C, et al. Effect of CT scanning parameters on volumetric measurements of pulmonary nodules by 3D active contour segmentation: a phantom study. Phys Med Biol 2008; 53: 1295-1312.

32. Tins B. Technical aspects of CT imaging of the spine. Insights Imaging 2010; 1: 349-359.

33. Schönström N. The significance of oblique cuts on CT scans of the spinal canal in terms of anatomic measurements. Spine 1988; 13: 435-436.

34. Schwarz T, Saunders J. CT acquisition principle. In: Schwarz T, Saunders J, editors. Veterinary computed tomography. Oxford: Wiley-Blackwell 2011; pg. 9–27.

35. Seiler G, Kinns J, Dennison S, et al. Vertebral column and spinal cord. In: Schwarz T, Saunders J, editors. Veterinary Computed Tomography. Oxford: Wiley-Blackwell; 2011. pg. 209-228.

36. Beers GJ, Carter A, Leiter B, Tilak S, Shah R. Interobserver discrepancies in distance measurements from lumbar spine CT scans. Am J Roentgenol 1985; 144: 395-398.

37. Passantino A. Application of the 3Rs principles for animals used for experiments at the beginning of the 21st century. Annu Rev Biomed Sci 2008; 10: T27-T32.

Table 1 Mean and standard deviation of morphometrical dimensions of thoracolumbar vertebral canal and dural sac in 5 normal adult sheep.

	TDS (mm)	SDS (mm)	ADS (mm²)	TVC (mm)	SVC (mm)	AVC (mm²)	PDSD (mm)	AES (mm²)	SAC (mm)
T1	11.3 ± 0.7^{a}	9.4 ± 1.6^{a}	84.9 ± 12.3^{a}	23.2 ± 3.0^{a}	15.4 ± 1.5^{a}	268.7 ± 12.2^{a}	4.4 ± 1.3^{a}	169.8 ± 42.1^{a}	6.0 ± 1.2^{a}
T2	8.7 ± 1.5^{a,d}	8.6 ± 1.7^{b}	48.7 ± 3.5^{a,b}	14.5 ± 1.3^{b,c}	11.2 ± 1.0^{a,b}	124.6 ± 9.7^{b,c,d}	2.2 ± 0.6^{b,c}	72.2 ± 13.0^{b}	2.8 ± 1.1^{b}
T3	7.5 ± 0.6^{b,c}	7.2 ± 0.4^{b}	41.4 ± 2.0^{b}	13.6 ± 1.3^{b,c}	10.8 ± 0.6^{a,b}	109.4 ± 4.1^{c,d,e}	1.8 ± 0.5^{b,c}	65.7 ± 7.2^{b}	3.5 ± 0.4^{a,b}
T4	7.3 ± 0.6^{b,c}	6.5 ± 0.8^{b}	42.8 ± 4.8^{b}	12.0 ± 1.3^{c}	10.1 ± 1.2^{b}	93.5 ± 12.4^{d,e}	1.6 ± 0,7^{b,c}	51.0 ± 10.6^{b}	3.6 ± 1.7^{a,b}
T5	6.0 ± 1.5^{c}	6.0 ± 1.4^{b}	38.5 ± 14.3^{b}	10.8 ± 2.7^{c,d}	8.8 ± 2.3^{b}	88.8 ± 6.7^{d,e}	1.4 ± 0,7^{b,c}	45.2 ± 12.0^{b}	3.3 ± 1.0^{a,b}
T6	6.8 ± 0.4^{b,c}	6.3 ± 0.7^{b}	41.1 ± 5.5^{b}	11.1 ± 1.0^{c,d}	10.1 ± 0.7^{b}	97.7 ± 10.1^{c,d,e}	0.9 ± 0.2^{c}	49.9 ± 10.8^{b}	3.8 ± 1.1^{a,b}
T7	6.9 ± 0.2^{b,c}	6.1 ± 0.4^{b}	41.5 ± 9.3^{b}	11.1 ± 1.3^{c,d}	9.5 ± 1.1^{b}	82.2 ± 15.6^{d,e}	1.3 ± 0.6^{b,c}	41.7 ± 17.9^{b}	3.3 ± 1.1^{a,b}
T8	6.9 ± 0.6^{b,c}	6.1 ± 0.5^{b}	40.7 ± 6.8^{b}	11.0 ± 1.1^{c,d}	9.7 ± 1.0^{b}	79.0 ± 14.9^{d,e}	1.2 ± 0.4^{b,c}	38.3 ± 17.5^{b}	3.5 ± 1.2^{a,b}
T9	6.8 ± 0.5^{b,c}	6.2 ± 0.6^{b}	40.0 ± 6,7^{b}	10.8 ± 0.8^{c,d}	9.3 ± 1.3^{b}	77.2 ± 14.5^{d,e}	1.1 ± 0.3^{b,c}	36.7 ± 16.9^{b}	3.1 ± .5^{b}
T10	7.1 ± 0.3^{c}	6.6 ± 0.4^{b}	35.7 ± 3.2^{b}	11.5 ± 0.4^{c,d}	8.9 ± 1.2^{b}	83.0 ± 13.5^{d,e}	1.4 ± 0.3^{b,c}	38.3 ± 16.9^{b}	2.4 ± 1.6^{b}
T11	6.9 ± 0.8^{b,c}	6.6 ± 0.3^{b}	39.3 ± 7.7^{b}	10.9 ± 0.9^{c,d}	9.5 ± 0.9^{b}	84.9 ± 13.2^{d,e}	1.1 ± 0.4^{b,c}	40.4 ± 18.4^{b}	2.9 ± 0.8^{b}
T12	6.7 ± 0.4^{c}	6,6 ± 0.3^{b}	39.4 ± 8.9^{b}	11.3 ± 0.9^{c,d}	9.2 ± 0.8^{b}	90.0 ± 9.0^{d,e}	1.4 ± 0.5^{b,c}	40.4 ± 16.1^{b}	2.6 ± 0.9^{b}
T13	7.2 ± 0.4^{b,c}	6,3 ± 0.4^{b}	39.4 ± 9.9^{b}	12.2 ± 0.4^{c,d}	9.2 ± 0.5^{b}	92.6 ± 8.0^{d,e}	1.4 ± 0.2^{b,c}	48.1 ± 15.1^{b}	2.9 ± 0.6^{b}
L1	6.8 ± 0.4^{b,c}	6.5 ± 0.7^{b}	42.2 ± 9.5^{b}	12.8 ± 0.6^{c,d}	9.1 ± 0.4^{b}	92.4 ± 5.8^{d,e}	1.9 ± 0.2^{b,c}	49.4 ± 17.3^{b}	2.5 ± 0.4^{b}
L2	7.0 ± 0.5^{b,c}	6.4 ± 0.5^{b}	43.7 ± 11.9^{b}	12.8 ± 0.5^{c,d}	9.6 ± 0.6^{b}	103.1 ± 10.3^{c,d,e}	1.8 ± 0.6^{b,c}	51.7 ± 19.4^{b}	3.2 ± 1.0^{b}
L3	7.1 ± 0.5^{b,c}	6.7 ± 0.3^{a,b}	45.6 ± 10.2^{a,b}	12.9 ± 0.6^{b,c}	9.7 ± 0.6^{b}	95.2 ± 8.3^{c,d,e}	1.7 ± 0.6^{b,c}	50.6 ± 22.7^{b}	3.0 ± 0.9^{a,b}
L4	7.6 ± 0.6^{b,c}	7.2 ± 0.8^{a,b}	54.1 ± 12.3^{a,b}	13.6 ± 0.8^{b,c}	10.7 ± 1.9^{a,b}	105.4 ± 7.2^{c,d,e}	1.8 ± 0.5^{b,c}	55.1 ± 21.0^{b}	3.7 ± 1.3^{a,b}
L5	8.5 ± 1.3^{a,b}	7.2 ± 1.2^{a,b}	58.6 ± 18.9^{a,b}	14.5 ± 2.7^{b,c}	10.6 ± 1.8^{a,b}	139.7 ± 16.9^{bc}	1.6 ± 0.4^{b,c}	64.8 ± 20.7^{b}	3.7 ± 0.9^{a,b}
L6	10.0 ± 1.1^{a,d}	7.5 ± 1.2^{a,b}	60.4 ± 12.4^{a,b}	19.1 ± 0.8^{d}	11.6 ± 1.2^{a,b}	167.0 ± 8.9^{b}	2.9 ± 0.6^{b}	85.8 ± 28.2^{a,b}	4.1 ± .8^{a,b}
F-test	18.611*	6.563*	6.623*	37.876*	10.773*	73.577*	9.891*	14.522*	2.654*

* $p < 0.001$; N.S. not significant; different superscript letters in the same column are significantly different ($p < 0.001$).

AES = Area of the epidural space. ADS = Area of the dural sac. AVC = Area of the vertebral canal. PDSD= Pedicle–dural sac distance. SAC= space available for dural sac. SDS = Sagittal diameter of the dural sac. SVC = Sagittal diameter of the vertebral canal. TDS = Transverse diameter of the dural sac. TVC = Transverse diameter of the vertebral canal.

Table 2 Correlations between the different dimensions of the vertebral canal and dural sac of the thoracolumbar vertebrae in 5 normal adult sheep

	TVC	SDS	ADS	TDS	SVC	AVC	PDSD	AES	SAC
TVC		0.782*	0.703*	0.824*	0.712*	0.829*	0.687	0.693	0.47
SDS			0.616	0.653	0.663	0.668	0.613	0.566	0.424
ADS				0.726*	0.666	0.738*	0.682	0.613	0.457
TDS					0.781*	0.948*	0.844*	0.855*	0.54
SVC						0.890*	0.612	0.814*	0.514
AVC							0.796*	0.929*	0.6
PDSD								0.727*	0.418
AES									0.558
SAC									

*Indicates $r > 0.7$ and $p < 0.001$.

AES = Area of the epidural space. ADS= Area of the dural sac. AVC= Area of the vertebral canal. PDSD= Pedicle–dural sac distance. SAC= space available for dural sac SDS= Sagittal diameter of the dural sac. SVC= Sagittal diameter of the vertebral canal. TDS= Transverse diameter of the dural sac. TVC= Transverse diameter of the vertebral canal.

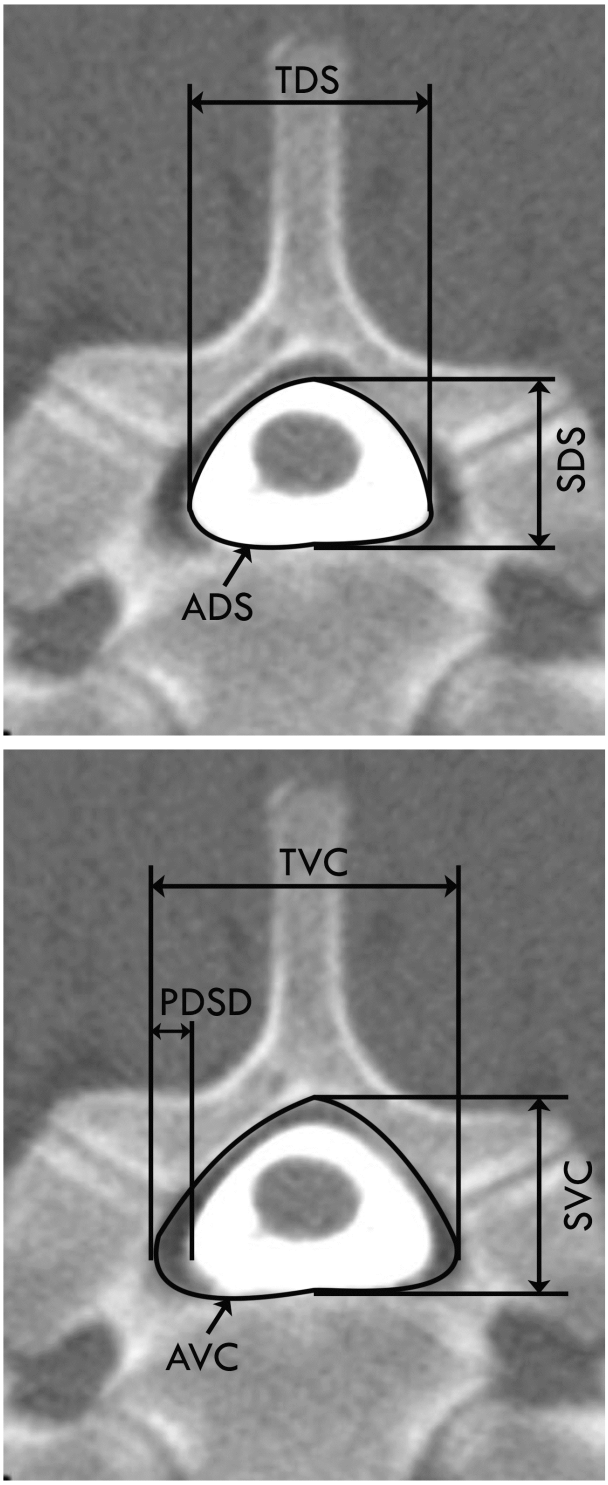

Figure 1 Transverse computed tomographic myelography image at the middle of T1 demonstrating the different measurements taken in this study. ADS = Area of the dural sac. AVC = Area of the vertebral canal. PDSD= Pedicle–dural sac distance. SDS = Sagittal diameter of the dural sac. SVC = Sagittal diameter of the vertebral canal. TDS = Transverse diameter of the dural sac. TVC = Transverse diameter of the vertebral canal.

4 Summary of Results and Discussion

4.1 Sheep as animal model for spinal research

A wide variety of implants and surgical procedures are available for treatment of spinal disorders. Prior to their clinical use in humans, implants must undergo rigorous testing both in vitro and in vivo to evaluate the biomechanical performance, biocompatibility, mechanical stability as well as their safety (PEARCE et al., 2007). For in vitro tests, spine specimens from human donors are preferably used in order to mimic the clinical situation as much as possible particularly when anatomy and size are important. However, there are some difficulties in using the human specimens such as the availability of fresh frozen human cadaver is very limited and heterogeneity in geometrical and mechanical properties (SMIT, 2002). Results of in vitro studies can be difficult to extrapolate to the in vivo situation. For instance, in vitro studies do not provide time-dependent changes of biomechanics, histological and functional behaviour after applying instruments (TOMINAGA et al., 1995).

Animal models are more easily available in all desired age groups, and have more uniform geometrical and biomechanical properties. For these reasons, the use of animal models is an alternative for testing of implants and surgical procedures prior to clinical use in humans.

An appropriate animal model for any research should be based on the following considerations: “1) appropriateness as an analogy, 2) transferability of information, 3) genetic uniformity of organisms where applicable, 4) background knowledge of biological properties, 5) cost and availability, 6) generalizability of the results, 7) ease and adaptability to experimental manipulation, 8) ecological considerations, and 9) ethical and societal implications” (DAVIDSON et al., 1987).

Various animals have been used as model for spinal research. (GURR et al., 1988; WALL et al., 1998; REID et al., 2002; GANEY et al., 2003). MARTINI and co-authors (2001) reported that rats, mice and rabbits were the most commonly used, 36%, 26% and 13% respectively, and attributed that to their lower cost and ease to handling. Because of their small size, their use was restricted mainly in preliminary orthopaedic studies such as cytocompatibility. They also reported that non-human primates and dogs were the dominant animal models. Non-human primates provide an excellent model due to their analogy with humans, but they are highly cost, difficult to handle, and could cause severe zoonotic diseases, as well as the ethical pressures of using this species. Dogs, as companying animals, are not well accepted to society as animal model. Nevertheless, the use of primates and dogs is decreasing in the European community due to the emotional impact related to these kinds of animals and to the legal aspects involved in their experimental use. Pigs show some physiological

similarities with human, but its rapid body growth and weight, and its difficult handling restrict its use in long-term orthopaedic experiments.

The sheep may be a useful model for bone related studies for many reasons (ZARRINKALAM et al., 2009): (1) the size and mechanical characteristics of the skeleton are comparable to humans which makes their large vertebral bodies more suited to conventional surgical procedures, (2) older sheep display Haversian bone remodelling; (3) they are genetically closer to humans than rodents and mice; (4) ewes ovulate spontaneously and have sex hormone profiles similar to women; (5) the oestrus cycle in sheep is almost continuous; (6) they are docile and easy to handle; (7) they are relatively inexpensive to maintain and are available in large numbers in most countries; (8) they usually present fewer ethical concerns than the use of domestic pets and non-human primates.

Because of the previously mentioned considerations, sheep are becoming popular animal models in orthopaedic research. The ideal animal model should mimic the anatomy, biomechanics, cell biology and pathological changes seen in the human skeleton (TURNER, 2001). Therefore, extensive comparative anatomical and biomechanical researches have been done with animal models to determine whether the animal spine is suitable as a representative model for the human spine.

WILKE et al. (1997b) documented sheep spine biomechanics to validate it as model for the human spine. They studied the range of motion (ROM), neutral zone and stiffness degree and compared the generated data with human published literatures. They stated that sheep spines are biomechanical similar to human. They also reported the flexion and extension ROM of thoracic spine ranged between 2-5°. In lumbar region increased slightly 4-6°. Generally, ROM in extension was larger than in flexion. In axial rotation, large motion was documented in cranial and middle thoracic spine, with values between 6° and 10°. The cranial thoracic vertebrae showed behaviour similar to that of the lumbar spine. The ROM at the level of T10-T11 decreased from 4.3° to the smallest values in caudal lumbar region (1.7° and 0.6°). The ROM in lateral flexion in thoracic and lumbar raged between 12.5° and 4°.

In the present study the use of a sheep spine as an alternative for human spine for conducting spine research is discussed from the morphometric point of view.

4.2 Materials and method

For a high quality morphometric study, an exact measurement method is indispensable. Sheep spinal dimensions have been measured in vitro using cadaveric specimens (WILKE et al., 1997a). Most of specimens used in vitro were dried or fixed in formalin and their dimensions may therefore no longer be identical with those before death, because of tissue

tend to shrink (EDMONDSTON et al., 1994). Furthermore, some preservation methods, such as freezing and formalin fixation, cause an alteration of bone biomechanical properties (LINDE et al., 1993; CURREY et al., 1995). In order to avoid the aforementioned disadvantages of preservation methods and obtain more accurate dimensions, the measurements should be taken from live subjects, which can be achieved through using modern diagnostic imaging tools such as computed tomography (CT). Computed tomography has been used in morphometric studies to depict normal size and shape of the human vertebral canal at various levels (HERZOG et al., 1991; SENEL et al., 1994). It enables additional measurements to be made in the transverse planes, which is cannot be done with the manual techniques using clipper or hand-held micrometer. Moreover, the measurements, which based on computerized imaging, are more accurate and reproducible than manual measuring method (ROSOL et al., 1996; TATAREK, 2005; FLYNN et al., 2007). The manual measuring methods were rounded to the nearest millimetre larger than actual dimension, which represents a potential measurement error of the order of 6–7% in measurements (TATAREK, 2005). Furthermore, the irregular shape of the bony surfaces may induce some variability and/or error when determining the dimensions of the vertebra (TATAREK, 2005; FLYNN et al., 2007).

The measurements' accuracy is the one of the most important aspect of the morphometric studies. Therefore, the factors affecting the accuracy should be addressed. The common factors degrade the measurements based on CT images are scanning parameters (WAY et al., 2008), post-processing and display setting (BEERS et al., 1985) and operator factors (BEERS et al., 1985; TINS, 2010).

For CT scan, animal should be anesthetized to minimize the effect of motion artefacts on the image quality as much as possible. The animal was anesthetized using a combination of atropine sulphate, butorphanol tartrate and midazolam as premedication agents and ketamine chlorhydrate as induction agent. At the time of this study this protocol was one of the most recommended anaesthetic regime for the sheep (KOZIOL, 2011).

The CT scanning parameters of this study were set up to minimize as much as possible the artefacts caused by motion which decrease the accuracy of the measurements by degrading the CT image quality and thus decrease the chance to detect the outline of region of interest. The motion artefacts could be minimized by shortening the scan time (high pitch and short tube rotation time) (SCHWARZ et al., 2011) and decreasing the respiratory motion, which achieved by positioning the animal in dorsal recumbency during scanning. Animal in the first part of this study (Publication 1) was positioned in sternal recumbency to preserve the spinal curvatures as much as possible for accurate measurements (i.e. disc thickness).

The terms “reconstruction” and “reformatting” are commonly used synonymously but they are a little bit different processes (TINS, 2010). Image reconstruction is the term describing the calculation of images from the raw data obtained from the detector modules of the CT scanner. Once image data has been reconstructed, the image data can be reformatted in any thickness and plane in real time (TINS, 2010).

The transverse and sagittal CT images, which reformatted using multi-planar reformation, are recommended to study the anatomical characteristics of the human vertebrae (GABRIEL, 2004). In this study, CT images were reformatted with slice thickness of 2 mm or less (except volumetric study – Publication 2), which consist with above mentioned study.

The volume average effect is post-processing artefact, which occurs when different objects are represented by the same voxel. Each object only partially fills the voxel and is therefore a partial volume. In order to minimize volume average effect, the slice thickness should be decreased (2 mm or less) (TINS, 2010). But reducing slice thickness is associated by high signal noise ratio, which in turns decreases the image quality. To overcome this dilemma, the mA should be increased (SCHWARZ et al., 2011), which set up on 200 mA in this study.

Image display setting also affects obviously the image quality by its influence on the signal noise ratio, where increasing the window width decreasing the noise level on the image, therefore it is recommended to display a thin slices with wide window setting. The scanning parameters in the current study are consistent with published spinal CT imaging protocol (SEILER, 2011).

In human, the myelography technique was first described by SICARD and FORESTIER (1921). By the end of the 1920s, it had become an established technique (WORTH, 1938; BONNEMAIN, 2000). In the seventies and eighties, the introduction of CT and water-soluble non-ionic contrast agents made the procedure easier to perform, safer and diagnostically more precise. Computed assisted myelography (CAM) was first published in 1976 by Di CHIRO and SCHELLINGER (1976) and it soon became a standard procedure. Then, MR imaging found its way into clinical routine, and over a short period, it made myelography look outdate. MRI seems to be the ideal tool for spinal imaging as it has some obvious advantages over myelography and CAM: non invasive, no radiation, no contrast agents, and excellent soft-tissue contrast (OZDOBA et al., 2011).

Modern MRI, however, is not automatically superior to myelography. In human, the nerve root compression is underestimated by MRI in nearly 30% of surgically confirmed cases compared to only 5 to 7% in myelography (BARTYNSKI et al., 2003). A recent study found myelography with CT “more reliable and reproducible than MRI” when deciding on which levels decompressive lumbar surgery should be performed (MORITA et al., 2011).

Furthermore, and especially important, in cases where surgery is considered, MRI tends to underestimate the width of the spinal canal and the foramina, thereby making spinal stenosis appear more severe than myelography and CAM (GRAMS et al., 2010; NAGANAWA et al., 2011). Another study compared MRI and CAM for quantitative evaluation of lumbar intracanalar cross-section and its results supported the previous findings, where its revealed that dural sac area was significantly smaller when measured by MR than by CAM (OGURA et al., 2011). Because of the previously mentioned considerations, the morphometrical analysis of dural sac in this study was based on CAM images.

The myelography protocol in the current study has been modified from that one used for large dog breeds. The contrast media dose of 0.45 ml/kg was sufficient to fill the subarachnoid space of the thoracolumbar spine. The lumbar puncture approach was selected to perform the myelography because it is safer and the amount of the contrast media is less than for cervical puncture, thus minimising its adverse effects.

The spinal needle was inserted between the dorsal spinal process of L5 and L6 perpendicular to the longitudinal axis of the vertebral body of L6. At this level the needle's trajectory is well marked with easily palpated landmarks, and thus reduce obviously the number of attempts at positioning the needle in the subarachnoid space (1-3 attempts per sheep). The length of the needle used in this study was 90 mm. The average distance required to contact the dorsal surface of the vertebral body was 59.3 ± 0.6 mm. This length was measured from the thoracolumbar fascia to the spinal canal floor. It has been reported that the skin is usually about 2 mm (BROWN et al., 2000; SEN et al., 2004). So, 90 mm needles should be adequate in most breeds, even in those with thick subcutaneous fat layer.

The Iopamidol was used as contrast agent in this study. Until the time of this works there was no documentation of the side effect of iopamidol for myelography in sheep. A study carried out in dogs to assess the iopamdiol revealed that the use of iopamidol 300 mgI/ml at 0.25 ml/kg during cervical myelography did not result in relevant cardiovascular and respiratory alterations (COX et al., 1986). Moreover, the sheep were recovered without clinically complications except a mild lameness in one sheep (Publication 3).

4.3 Results

The results of the sheep thoracolumbar spine morphometry (Publication 1) confirmed the hypothesis that the dimensions of the lumbar spine are larger than thoracic one. The results highlighted that the vertebral bodies were wider than deep, most obviously in the lumbar vertebrae. The spinal canal has a similar behaviour like vertebral bodies, while it tends to have nearly an equal width and depth at the caudal thoracic region. The intervertebral discs

were thicker in the lumbar than in the thoracic spine. The pedicles were higher and longer than they were wide over the entire thoracolumbar spine.

From this point of view, the vertebral column composed of 2 unequal pyramid regions (T2-T8 and L2-L5) connected thought trapezoid region (T9-L1). This finding challenges the results of WILKE et al (1997b), in which the vertebral dimensions (particularly the vertebral body) continuously increase toward caudal. The concept of the unequal pyramidal shapes may be explained biomechanically. WILKE et al (1997a) documented the biomechanical properties of sheep functional spinal units and their results revealed that the T6-T7spine units followed by L1-L2 had the highest flexion and extension range of motion between T2 and L5, where they represent the apex of the pyramid regions.

The current study compared the sheep lumbar spine to human but not the thoracic vertebrae. It could be explained in two reasons. Firstly, most of the experimental spinal research carried out on sheep lumbar region particularly for training purposes (TURAN SUSLU et al., 2012). Secondly, the biomechanics of lumbar is very similar to human than thoracic spine (WILKE et al., 1997a).

The absolute values comparison of the lumbar vertebrae between the sheep and human revealed several differences. The human vertebrae were wider and deeper than those of sheep, as much as 17.1 mm (40.6%) and 14.7 mm (45.1%), respectively. In contrast, sheep lumbar vertebrae were longer than human ones, as much as 10.5 mm (28.5%). In both species, the spinal canal was wider than it was deep and increased in width towards the caudal vertebral level. The human spinal canal was wider and deeper than sheep, as much as 10.6 mm (42.7%) and 8.4 mm (45%) respectively. The pedicles in both species were higher than they were wide. Sheep pedicles were higher and had a greater lateral inclination than humans, where the latter had a wider and greater pedicle axis length than sheep. The spinal indices comparison showed a good similarity to human in terms of the vertebral endplates and spinal canal, which confirmed the hypothesis that the sheep lumbar vertebrae are comparable to human based on morphometric point of view (Publication 2). Generally the human's lumbar vertebrae were larger than sheep particularly the width and depth of the end-plates, which increased more caudally in the human spine, likely because of the upright position. The human spine demands relatively larger caudal vertebral bodies to balance the higher longitudinal loads (BUSSCHER et al., 2010). This was also probably the explanation for the thicker intervertebral discs observed in the human spine in this study, which were up to 69.5% (6.4 mm) as thick as the sheep disc in the lumbar region. Another difference between human and ovine lumbar spines is the curvature, which for the sheep is slightly kyphotic rather than lordotic due to the interlocking mechanism of the facet articulation (DATH et al., 2007).

One of the main objectives of this study was to obtain quantitative morphometric data on sheep dural sac, and determine the presence of correlations between the measures. The results revealed that the sagittal diameters of the dural sac ranging from 5.1 to 12.0 mm. Transverse diameters ranged from 5.6 to 12.2 mm. The dural sac area covered 45.9% and 49.0% of the thoracic and lumbar vertebral canal transverse area. The dural sac area was significantly positive correlated with the transverse diameter and area of the vertebral canal.

As secondary objective, the relationship between the dural sac and its surrounding vertebral bony structures was documented, where this relationship play an important role when using sheep spine as model for preclinical testing of spinal implants. The results showed that the pedicle-dural sac distance in the lumbar vertebrae was up to 15.8% larger than in the thoracic ones. The clinical relevance of this finding is the lumbar vertebrae are safer than the thoracic ones for application of spinal implants, which confirmed the hypothesis (publication 3).

4.4 Study limitations

One limitation of this study was the small sample size. Regards to the 3Rs principles (**R**eplacement, **R**eduction and **R**efinement) (PASSANTINO, 2008), the number of the animals involved in the study should be as low as possible. In the current study, 5 animals were used for publication 1 and a similar number for publication 3. The number of 5 animals was the lowest possible to comply with the rules of 3Rs, but sufficient enough to provide reliable data. However, the repeatability of the sheep dimensions and small variance around the mean indicated that a larger sample was not necessary. Moreover, previous investigators used similar sample sizes for similar studies (WILKE et al., 1997a; WILKE et al., 1997b; KUMAR et al., 2000; MCLAIN et al., 2002; RILEY et al., 2004). In order to overcome the influence of the small sample size on the generated data, the significance level must be set at small p value ($P<0.003$; statistical value of 0.05 divided by 19 vertebrae) as recommended in the literatures (MASHARAWI et al., 2007). In this study, the p value has been set up even smaller ($P<0.0001$ and 0.001 for Publication 1 and 3 respectively).

The accuracy of the linear and transverse area measurements based on the CT images has not been tested in this study, because it was not one of its aims. JONES et al. (1995) studied the morphometry of the lumbosacral spine of dogs using CT. To validate their results, they tested the accuracy of CT measurements using a phantom (syringe filled with diluted contrast agent). Their results revealed that the accuracy of CT measurements was 100% for sagittal and transversal plane and was 85% for transverse area. Noteworthy the phantom's diameters were 5x5 mm. Some measurements in the current study was > 5-mm, such as

cortical bone thickness and disc thickness. Therefore the accuracy of these parameters is questionable.

For comparison of the lumbar vertebrae morphometry of both species, the human morphometric data were collected from the published literature rather than using identical measuring and scanning protocol like the sheep. Therefore, the comparison could be questionable. In this study, the spinal indices were used, which were calculated as the ratio between the vertebral dimensions, to rule out the heterogeneity of measuring methods and thus making the comparative results more reliable. Furthermore, most of human spine data, which were included in this work, were obtained using CT scanning as measuring method (WOLF et al., 2001; ODACI et al., 2003; ABUZAYED et al., 2010).

5 Zusammenfassung

Mahmoud Mageed

Morphometrische Untersuchung der thorakolumbalen Wirbelsäule von Schafen mittels Computertomographie und der Vergleich mit dem menschlichen Korrelat

Chirurgische Tierklinik der Veterinärmedizinischen Fakultät der Universität Leipzig

Eingereicht im März 2014
73 Seiten, 3 Publikationen, 128 Literaturangaben,
Schlüsselwörter: Schafe, Wirbelsäule Modell, Wirbelkörper Morphometrie, Wirbelkörper Volumen, Duralsack.

Schafe werden häufig als Tiermodell für In-vivo-Versuche verwendet, um neue Wirbelsäulenimplantate sowie chirurgische Prozeduren zu testen. Daher ist die umfassende Kenntnis der präzisen Morphometrie und der biomechanischen Merkmale der Schafwirbelsäule entscheidend für das experimentelle Design und die Interpretation der Ergebnisse in den Studien. Es sind wenige Daten über die Schafwirbelsäule bekannt. Auf Grund dessen zielt die aktuelle Studie darauf ab, mehr Wissen über die Morphometrie der thorakolumbalen Wirbelsäule von Schafen zu gewinnen.

Der erste Teil dieser Studie soll die Morphometrie der Brust- und Lendenwirbelsäule dokumentieren. Das Ziel besteht darin, die Verwendung von Schaflendenwirbeln als Modell für die menschliche Wirbelsäule im morphometrischen Vergleich beurteilen zu können. Aus diesem Grund wurden Computertomographische Untersuchungen (CT) von fünf klinisch gesunden weiblichen Merino-Schafen (2 Jahre, 62 kg ± 5,3 kg) unter Allgemeinanästhesie durchgeführt. Die CT-Bilder wurden mit einer Schichtdicken von 1 mm aus T2 bis L6 gewonnen. Anschließend wurden die CT-Bilder in der transversalen und sagittalen Ebene multiplanar reformatiert. Danach wurden Messungen und Bewertungen mit einer geeigneten Software an den Wirbelkörpern, Wirbelkanälen, Bandscheiben und Pedikeln durchgeführt. Basierend auf den erzeugten morphometrischen Daten der Schaflendenwirbel wurden vier Wirbelsäulen-Indizes und Pavlov's-ratio sowie das Volumen der Wirbelkörper berechnet. Die Wirbelsäulen-Indizes stellten den Konkavitäts-, Endplatten-, Spinalkanal- und Pedikel-Index dar. Für die Messung des Volumens von Wirbelkörpern wurden die transversalen CT-Daten in 5 mm Schichtdicke formatiert und in geeignete Software eingefügt. Danach wurden die vier Indizes-Wirbelsäulen und das Volumen der Lendenwirbelkörper mit den veröffentlichten Daten von menschlichen Wirbeln verglichen. Sie wurden als „vergleichbar" definiert, wenn das Verhältnis Schaf-Mensch jedes einzelnen Wirbels Variationen von weniger als 20 % aufwies.

Der zweite Teil der vorliegenden Arbeit hat zum Ziel, quantitative morphometrische Daten des thorakolumbalen Duralsacks zu ermitteln. Weiterhin sollen die anatomischen Beziehungen zwischen dem Duralsack und seinen umliegenden knöchernen Strukturen der Wirbelsäule beschrieben werden. Dazu wurden CT-Myelographien an fünf erwachsenen weiblichen Schwarzkopfschafen (2 Jahre ± 0,4 Jahre, 80,6 kg ± 28,7 kg) unter Allgemeinanästhesie durchgeführt. Transversale CT-Bilder wurden mit 2 mm Schichtdicke von T1 bis L6 gemessen. Sagittal- und Transversal-Durchmesser sowie die Querschnittsfläche von Duralsack und Wirbelkanal wurden auf CT-Bildern gemessen. Um die anatomische Beziehung zwischen dem Duralsack und den knöchernen Strukturen des Wirbelkanals zu ermitteln, wurden der Pedikel-Duralsack-Abstand und das Platzangebot für den Duralsack berechnet.

Die Wirbelkörper und der Wirbelkanal der ovinen thorakolumbalen Wirbelsäule sind breiter als tief, vor allem im Bereich der Lendenwirbel. Die Bandscheiben sind in der Lendenwirbelsäule 57,4 % dicker als in der Brustwirbelsäule. Die Pedikel der Brust- und Lendenwirbelsäule waren höher und länger als breit. Im Vergleich zum Menschen ist das Volumen von Schaflendenwirbelkörpern 48,6 % kleiner. Der Vergleich der absoluten Werte zwischen den beiden Spezies ergab, dass Schafe kleinere, längere und schmalere Wirbelkörper, dünnere Bandscheiben, einen schmaleren Spinalkanal und schmalere, höhere Pedikel besitzen. Der Vergleich der Wirbelsäulen-Indizes zeigte eine gute Vergleichbarkeit mit menschlichen Wirbelendplatten und Wirbelkanälen.

Im zweiten Teil der Studie konnte festgestellt werden, dass die Duralsackfläche 45,9 % des Brustwirbelkanals und 49,0 % des Lendenwirbelkanals einnimmt. Die Duralsackfläche korreliert deutlich positiv mit dem Querdurchmesser und der Fläche des Wirbelkanals. Der Pedikel-Duralsack-Abstand in der Lendenwirbelsäule war bis zu 15,8 % größer als in der Brustwirbelsäule.

Die Schaflendenwirbelsäule weist in Bezug auf die Wirbelendplattenregionen und den Wirbelkanal eine hohe Ähnlichkeit mit der Wirbelsäule des Menschen auf. Das Schafwirbelsäulenmodell ist damit für das Studium künstlicher Bandscheiben sowie der Implantation von Bandscheibenverbindungsvorrichtungen geeignet. Die Dimensionen der Implantate müssen den Schaf-Pedikeln angepasst werden, um diese Tiere als Model für Implantate beim Menschen nutzen zu können. Der Lendenwirbelkanal ist sicherer zur Erprobung neuer Wirbelsäulenimplantate, da dieser mehr Platz für den Duralsack im Vergleich zur Brustwirbelsäule aufweist.

6 Summary

Mahmoud Mageed

Morphometric analysis of the sheep thoracolumbar spine using computed tomography and a comparison with the human correlate

Large Animal Clinic for Surgery, Faculty of Veterinary Medicine, University of Leipzig

Submitted in March 2014

73 pages, 3 publications, 128 references.

Keywords: sheep, spinal model, vertebral morphometry, vertebral volume, dural sac

Sheep are commonly used as animal model for in vivo testing of new spinal implants as well as surgical procedures. Therefore, extensive knowledge of the precise morphometry and biomechanics features of sheep spine is crucial for experimental design and interpretation of results obtained in these trials. Little is known about the sheep spine. Therefore, the current study, which comprises of two parts, aimed to gain more knowledge concerning the morphometry of sheep thoracolumbar spine.

The first part aimed to document the morphometry of the sheep thoracolumbar vertebrae and to assess the feasibility of using sheep lumbar vertebrae as a model for human spine researches based on morphometric comparison. For this reason, computed tomographic (CT) scanning was carried out in five clinically healthy female Merino sheep (2 years, 62 ± 5.3 kg) under general anaesthesia. CT images were reformatted with 1-mm slice thickness from T2 through L6. The CT images were reformatted in transverse and sagittal planes using multiplaner reconstruction algorithm. Subsequently, CT images were transferred to a workstation and reviewed with dedicated software for measuring the dimensions of the vertebral bodies, spinal canal, intervertebral disc, and pedicles. Based on the generated morphometric data of the sheep lumbar vertebrae, four spinal indices and Pavlov's ratio were calculated as well as the volume of the vertebral bodies. The spinal indices were concavity index, endplate index, spinal canal index and pedicle index. For measuring vertebral body volume, the transverse CT data were reformatted in 5-mm slice thickness and imported in dedicated software. Thereafter, the four spinal indices and the volume were compared to human published data. The parameter was defined comparable if the ratio sheep/human of each individual vertebra showed variation less than 20%.

The second part of the current work aimed to provide quantitative morphometric data of the thoracolumbar dural sac and describe the anatomical relationship between the dural sac and its surrounding osseous structures of the spine. To achieve these aims, computed assisted

myelography was carried out in five adult female blackhead sheep (2.0 ± 0.4 years, 80.6 ± 28.7 kg) under general anaesthesia. Transverse images were acquired with 2-mm slice thickness from T1 to L6. Sagittal and transverse diameters and cross-sectional area of the dural sac and the spinal canal were measured on CT images. To determine the anatomical relationship between the dural sac and osseous structures of spinal canal, the pedicle-dural sac distance and available space for dural sac were calculated.

The morphometric data showed that the sheep thoracolumbar vertebral bodies and the spinal canal were wider than they were deep, most obviously in the lumbar vertebrae. The intervertebral discs were as much as 57.4% thicker in the lumbar than in the thoracic spine. The pedicles were higher and longer than they were wide over the entire thoracolumbar spine. Compared to humans, sheep lumbar vertebral body volumes were 48.6% smaller. The comparison of absolute values between both species revealed that sheep had smaller, longer and narrower vertebral bodies, thinner intervertebral discs, narrower spinal canal and narrower, higher pedicles. The comparison of the spinal indices showed a good comparability to human in terms of the vertebral endplate and spinal canal.

The results of the second parts showed that the dural sac area covered 45.9% and 49.0% of the thoracic and lumbar vertebral canal area, respectively, and it is significantly (positive) correlated with the transverse diameter as well as area of the vertebral canal. The pedicle-dural sac distance in the lumbar vertebrae was up to 15.8% larger than in the thoracic ones.

The clinical relevance of the current study, the sheep lumbar spine has good comparability to that of humans in terms of the vertebral endplate regions and spinal canal, suggesting that a sheep spinal model would be appropriate for studying artificial intervertebral discs, implantation of intervertebral fusion, etc. With regard to sheep pedicles, can be used as a model for spinal implant conditioned by adaptation of implant size to sheep pedicel dimensions. The lumbar vertebral canal shows more space for the dural sac, which seems to be safer for testing fixation spinal implants.

7 References

Abuzayed, B, Tutunculer, B, Kucukyuruk, B, Tuzgen, S. Anatomic basis of anterior and posterior instrumentation of the spine: morphometric study. Surg Radiol Anat. 2010;32:75-85.

Aebli, N, Goss, BG, Thorpe, P, Williams, R, Krebs, J. In vivo temperature profile of intervertebral discs and vertebral endplates during vertebroplasty: an experimental study in sheep. Spine. 2006;31:1674-78.

Ahlgren, BD, Lui, W, Herkowitz, HN, Panjabi, MM. Effect of anular repair on the healing strength of the intervertebral disc: a sheep model. Spine. 2000;25:2165-70.

Arlien-Søborg, P, Kjaer, L, Praestholm, J. Myelography, CT, and MRI of the spinal canal in patients with myelopathy: a prospective study. Acta Neurol Scand. 1993;87:95-102.

Ashman, R, Bechtold, J, Edwards, W, Johnston 2nd, C, McAfee, PC, Tencer, A. In vitro spinal arthrodesis implant mechanical testing protocols. J Spinal Disord. 1989;2:274-81.

Azar-Kia, B, Fine, M, Naheedy, MH. Importance of metrizamide CT for evaluation of the thoracic spine. Comput Radiol. 1985;9:233-41.

Badami, JP, Norman, D, Barbaro, NM, Cann, CE, Weinstein, P, Sobel, D. Metrizamide CT myelography in cervical myelopathy and radiculopathy: correlation with conventional myelography and surgical findings. Am J Roentgenol. 1985;144:675-80.

Bartynski, WS, Lin, L. Lumbar root compression in the lateral recess: MR imaging, conventional myelography, and CT myelography comparison with surgical confirmation. Am J Neuroradiol. 2003;24:348-60.

Beers, GJ, Carter, A, Leiter, B, Tilak, S, Shah, R. Interobserver discrepancies in distance measurements from lumbar spine CT scans. Am J Roentgenol. 1985;144:395-8.

Bergmann, G, Graichen, F, Rohlmann, A. Hip joint forces in sheep. J Biomech. 1999;32:769-77.

Bland, MJ, Altman, DG. Statistical methods for assessing agreement between two methods of clinical measurement. lancet. 1986;327:307-10.

Böckler, D, Kotelis, D, Kohlhof, P, von Tengg-Kobligk, H, Mansmann, U, Zink, W, HÖMER, C, Ortlepp, I, Habel, A, Kauczor, H-U. Spinal cord ischemia after endovascular repair of the descending thoracic aorta in a sheep model. Eur J Vasc Endovasc Surg. 2007;34:461-9.

Bolender, N, Schönström, N, Spengler, D. Role of computed tomography and myelography in the diagnosis of central spinal stenosis. J Bone Joint Surg Am. 1985;67:240-46.

Bonnemain, B. L'huile iodée (lipiodol) en radiologie. Les premières années d'expérience: 1921-1931. Revue d'histoire de la pharmacie. 2000;88:493-508.

Brown, D, Wolcott, M, Crook, B. The measurement of skin thickness in Merino sheep using real time ultrasound. Wool Tech Sheep Bree. 2000;48:269-76.

Busscher, I, Ploegmakers, JJ, Verkerke, GJ, Veldhuizen, AG. Comparative anatomical dimensions of the complete human and porcine spine. Eur Spine J. 2010;19:1104-14.

Cain, CC, Fraser, RD. Bony and vascular anatomy of the normal cervical spine in the sheep. Spine. 1995;20:759-64.

COX, FH, Jakovljevic, S. The use of iopamidol for myelography in dogs: a study of twenty seven cases. J Small Anim Pract. 1986;27:159-65.

Currey, JD, Brear, K, Zioupos, P, Reilly, GC. Effect of formaldehyde fixation on some mechanical properties of bovine bone. Biomaterials. 1995;16:1267-71.

Da Costa, RC, Echandi, RL, Beauchamp, D. Computed tomography myelographic findings in dogs with cervical spondylomyelopathy. Vet Radiol Ultrasound. 2012;53:64-70.

Dath, R, Ebinesan, A, Porter, K, Miles, A. Anatomical measurements of porcine lumbar vertebrae. Clin Biomech. 2007;22:607-13.

Davidson, M, Lindsey, J, Davis, J. Requirements and selection of an animal model. Isr J Med Sci. 1987;23:551-55.

Denoix, J. Spinal biomechanics and functional anatomy. Vet Clin North Am Equine Pract. 1999;15:27-60.

Di Chiro, G, Schellinger, D. Computed tomography of spinal cord after lumbar intrathecal introduction of metrizamide (computer-assisted myelography). Radiology. 1976;120:101-04.

Edmondston, S, Singer, K, Day, R, Breidahl, P, Price, R. Formalin fixation effects on vertebral bone density and failure mechanics: An in-vitro study of human and sheep vertebrae. Clin Biomech. 1994;9:175-9.

Egermann, M, Goldhahn, J, Schneider, E. Animal models for fracture treatment in osteoporosis. Osteoporos Int. 2005b;16:129-38.

Eggli, S, Schlapfer, F, Angst, M, Witschger, P, Aebi, M. Biomechanical testing of three newly developed transpedicular multisegmental fixation systems. Eur Spine J. 1992;1:109-16.

F McLain, R, Yerby, SA, Moseley, TA. Comparative morphometry of L4 vertebrae: comparison of large animal models for the human lumbar spine. Spine. 2002;27:E200-6.

Flynn, JR, Bolton, PS. Measurement of the vertebral canal dimensions of the neck of the rat with a comparison to the human. Anat Rec. 2007;290:893-9.

Frigon, A. The Cat Model of Spinal Cord Injury. eds. Animal Models of Spinal Cord Repair. Springer; 2013, p.159-83.

Gabriel, P. Experimentelle Studie zum Vergleich der Bildqualität von axialen Schnittbildern und multiplanaren Reformationen der Computertomographie anhand von Wirbelkörperpräparaten. Röntgendiagnostik.,[Dissertation med]. Breisgau: Univ. Albert-Ludwigs-Universität; 2004.

Ganey, T, Libera, J, Moos, V, Alasevic, O, Fritsch, KG, Meisel, HJ, Hutton, WC. Disc chondrocyte transplantation in a canine model: a treatment for degenerated or damaged intervertebral disc. Spine 2003;28:2609-20.

Goel, VK, Panjabi, MM, Patwardhan, AG, Dooris, AP, Serhan, H. Test protocols for evaluation of spinal implants. J Bone Joint Surg Am. 2006;88:103-09.

Grams, AE, Gempt, J, Förschler, A. Comparison of spinal anatomy between 3-Tesla MRI and CT-myelography under healthy and pathological conditions. Surg Radiol Anat. 2010;32:581-85.

Gurr, KR, McAfee, PC, Shih, CM. Biomechanical analysis of anterior and posterior instrumentation systems after corpectomy. A calf-spine model. J Bone Joint Surg Am. 1988;70:1182-91.

Gurwitz, GS, Dawson, JM, McNamara, MJ, Federspiel, CF, Spengler, DM. Biomechanical analysis of three surgical approaches for lumbar burst fractures using short-segment instrumentation. Spine. 1993;18:977-82.

Hara, Y, Tagawa, M, Ejima, H, Orima, H, Fujita, M. Usefulness of computed tomography after myelography for surgery on dogs with cervical intervertebral disc protrusion. J Vet Med Sci. 1994;56:791-4.

Haussler, KK. Anatomy of the thoracolumbar vertebral region. Vet Clin North Am Equine Pract. 1999;15:13-26.

Herzog, RJ, Wiens, JJ, Dillingham, MF, Sontag, MJ. Normal cervical spine morphometry and cervical spinal stenosis in asymptomatic professional football players. Plain film radiography, multiplanar computed tomography, and magnetic resonance imaging. Spine 1991;16:S178-86.

Hirabuki, N, Mitomo, M, Miura, T, Hashimoto, T, Kawai, R, Kozuka, T. Computed tomographic myelography characteristics of spinal cord atrophy in juvenile muscular atrophy of the upper extremity. Eur J Radiol. 1991;13:215-9.

Høy, K, Hansen, ES, He, S-Z, Søballe, K, Henriksen, TB, Kjølseth, D, Hjortdal, V, Bünger, C. Regional blood flow, plasma volume, and vascular permeability in the spinal cord, the dural sac, and lumbar nerve roots. Spine. 1994;19:2804-11.

Inoue, H, Ohmori, K, Takatsu, T, Teramoto, T, Ishida, Y, Suzuki, K. Morphological analysis of the cervical spinal canal, dural tube and spinal cord in normal individuals using CT myelography. Neuroradiology. 1996;38:148-51.

Inufusa, A, An, HS, Lim, TH, Hasegawa, T, Haughton, VM, Nowicki, BH. Anatomic changes of the spinal canal and intervertebral foramen associated with flexion-extension movement. Spine. 1996;21:2412-20.

Jahng, TA, Fu, TS, Kim, DH. Open versus endoscopic lumbar pedicle screw fixation and posterolateral fusion in a sheep model: a feasibility study. Spine J. 2004;4:519-26.

Jones, J, Wright, J, Bartels, J. Computed tomographic morphometry of the lumbosacral spine of dogs. Am J Vet Res. 1995;56:1125-32.

Kadioglu, H, Takci, E, Levent, A, Arik, M, Aydin, I. Measurements of the lumbar pedicles in the Eastern Anatolian population. Surg Radiol Anat. 2003;25:120-26.

Kiefer, A, Parnianpour, M, Shirazi-Adl, A. Stability of the human spine in neutral postures. Eur Spine J. 1997;6:45-53.

Konrad, P, Tacker, W, Levy, W, Reedy, D, Cook, J, Geddes, L. Motor evoked potentials in the dog: effects of global ischemia on spinal cord and peripheral nerve signals. Neurosurgery. 1987;20:117-24.

Koziol M. Quantitative research on the development of pulmonary reactions in sheep resulting from administration of the α2-receptoragonist xylazine. [Dissertation med. vet]. Leipzig: Univ. Leipzig; 2011.

Krag, MH, Weaver, DL, Beynnon, BD, Haugh, LD. Morphometry of the thoracic and lumbar spine related to transpedicular screw placement for surgical spinal fixation. Spine. 1988;13:27-32.

Kumar, N, Kukreti, S, Ishaque, M, Mulholland, R. Anatomy of deer spine and its comparison to the human spine. Anat Rec. 2000;260:189-203.

Lehmann, W, Ushmaev, A, Ruecker, A, Nuechtern, J, Grossterlinden, L, Begemann, P, Baeumer, T, Rueger, J, Briem, D. Comparison of open versus percutaneous pedicle screw insertion in a sheep model. Eur Spine J. 2008;17:857-63.

Limthongkul, W, Karaikovic, EE, Savage, JW, Markovic, A. Volumetric analysis of thoracic and lumbar vertebral bodies. Spine J. 2010;10:153-8.

Linde, F, Sørensen, HCF. The effect of different storage methods on the mechanical properties of trabecular bone. J Biomech. 1993;26:1249-52.

Louis, R. Fusion of the lumbar and sacral spine by internal fixation with screw plates. Clin Orthop. 1986;203:18-33.

Mageed, M, Berner, D, Hohaus, C, Jülke H, Brehm, W, Gerlach, K, Morphometrical dimensions of the sheep thoracolumbar vertebrae as seen on digitised CT images. Lab Anim Res. 2013; 29:138-47.

Mann, NH, Brown, MD, Enger, I. Statistical diagnosis of lumbar spine disorders using computerized patient pain drawings. Comput Biol Med. 1991;21:383-97.

Manunta, ML, Careddu, GM, Masala, G, Columbano, N, Doria, C, Crissantu, L, Sanna Passino, E. Lumbar interbody expanding cage. A preliminary study on an animal model. Vet Comp Orthop Traumatol. 2008;21:382-4.

Martini, L, Fini, M, Giavaresi, G, Giardino, R. Sheep model in orthopedic research: a literature review. Comp Med. 2001;51:292-9.

Masharawi, Y, Salame, K, Mirovsky, Y, Peleg, S, Dar, G, Steinberg, N, Hershkovitz, I. Vertebral body shape variation in the thoracic and lumbar spine: characterization of its asymmetry and wedging. Clin Anat. 2007;21:46-54.

McLain, RF, Yerby, SA, Moseley, TA. Comparative morphometry of L4 vertebrae: comparison of large animal models for the human lumbar spine. Spine. 2002;27:E200-6.

Merzin, M. Applying stereological method in radiology: Volume measurement. [Dissertation Bachelor Physics], Tartu, Univ. of Tartu. 2008.

Mitchell, B, Williams, J. Respiratory function changes in sheep associated with lying in lateral recumbency and with sedation by xylazine. Vet Anaesth Analg. 1976;6:30-6.

Moore, RJ, Osti, OL, Vernon-Roberts, B, Fraser, RD. Changes in endplate vascularity after an outer anulus tear in the sheep. Spine. 1976;17:874-8.

Morita, M, Miyauchi, A, Okuda, S, Oda, T, Iwasaki, M. Comparison between MRI and myelography in lumbar spinal canal stenosis for the decision of levels of decompression surgery. J Spinal Disord Tech. 2011;24:31-6.

Naganawa, T, Miyamoto, K, Ogura, H, Suzuki, N, Shimizu, K. Comparison of magnetic resonance imaging and computed tomogram-myelography for evaluation of cross sections of cervical spinal morphology. Spine. 2011;36:50-6.

Newman, E, Turner, A, Wark, J. The potential of sheep for the study of osteopenia: current status and comparison with other animal models. Bone. 1995;16:S277-84.

Nout, Y, Reed, S. Cervical vertebral stenotic myelopathy. Equine Vet Educ. 2003;15:212-23.

Nout, YS, Rosenzweig, ES, Brock, JH, Strand, SC, Moseanko, R, Hawbecker, S, Zdunowski, S, Nielson, JL, Roy, RR, Courtine, G. Animal models of neurologic disorders: a nonhuman primate model of spinal cord injury. Neurotherapeutics. 2012;9:380-92.

Nunamaker, D. Experimental models of fracture repair. Clin Orthop Relat Res. 1998;(355 Suppl):56-65.

Odaci, E, Sahin, B, Sonmez, OF, Kaplan, S, Bas, O, Bilgic, S, Bek, Y, Ergür, H. Rapid estimation of the vertebral body volume: a combination of the Cavalieri principle and computed tomography images. Eur J Radiol. 2003;48:316-26.

Ogura, H, Miyamoto, K, Fukuta, S, Naganawa, T, Shimizu, K. Comparison of magnetic resonance imaging and computed tomography-myelography for quantitative evaluation of lumbar intracanalar cross-section. Yonsei med J. 2011;52:137-44.

Olsewski, J, Simmons, E, Kallen, F, Mendel, F, Severin, C, Berens, D. Morphometry of the lumbar spine: anatomical perspectives related to transpedicular fixation. J Bone Joint Surg Am. 1990;72:541-9.

Ozdoba, C, Gralla, J, Rieke, A, Binggeli, R, Schroth, G. Myelography in the Age of MRI: Why We Do It, and How We Do It.Radiol Res Pract. 2011;2011-7.

PASSANTINO A. Application of the 3Rs principles for animals used for experiments at the beginning of the 21st century. Annu Rev Biomed Sci. 2008;10:T27-T32.

Pavlov, H, Torg, J, Robie, B, Jahre, C. Cervical spinal stenosis: determination with vertebral body ratio method. Radiology. 1987;164:771-5.

Pearce, A, Richards, R, Milz, S, Schneider, E, Pearce, S. Animal models for implant biomaterial research in bone: a review. Eur Cell Mater. 2007;13:1-10.

Perretta, G. Non-human primate models in neuroscience research. Scand. J. Lab. Anim. Sci. 2009;36:77-85.

Pluijm, S, Tromp, A, Smit, J, Deeg, D, Lips, P. Consequences of vertebral deformities in older men and women. J Bone Miner Res. 2000;15:1564-72.

Putz, RLV, Müller□Gerbl, M. The vertebral column—a phylogenetic failure? A theory explaining the function and vulnerability of the human spine. Clini Anat. 1996;9:205-12.

Reid, JE, Meakin, JR, Robins, SP, Skakle, JM, Hukins, DW. Sheep lumbar intervertebral discs as models for human discs. Clin Biomech 2002;17:312-4.

Riley, LH, Eck, JC, Yoshida, H, Koh, YD, You, JW, Lim, TH. A biomechanical comparison of calf versus cadaver lumbar spine models. Spine. 2004;29:E217-20.

Roberts, R, Selcer, B. Myelography and epidurography. The Veterinary clinics of North America. J Small Anim Prac. 1993;23:307-29.

Rosol, M, Cohen, GL, Halpern, EF, Chew, FS, Kattapuram, SV, Palmer, WE, Dupuy, DE, Rosenthal, DI. Vertebral morphometry derived from digital images. Am J Roentgenol. 1996;167:1545-9.

Rossignol, S, Chau, C, Giroux, N, Brustein, E, Bouyer, L, Marcoux, J, Langlet, C, Barthélemy, D, Provencher, J, Leblond, H. The cat model of spinal injury. Prog Brain Res. 2002;137:151-68.

Roy-Camille, R, Saillant, G, Mazel, C. Internal fixation of the lumbar spine with pedicle screw plating. Clin Orthop Relat Res. 1986;7-17.

Schimandle, JH, Boden, SD. Spine update animal use in spinal research. Spine. 1994;19:2474-7.

Schönström, N. The significance of oblique cuts on CT scans of the spinal canal in terms of anatomic measurements. Spine. 1988;13:435-6.

Schönström, N, Lindahl, S, Willén, J, Hansson, T. Dynamic changes in the dimensions of the lumbar spinal canal: an experimental study in vitro. J Orthop Res. 1989;7:115-21.

Schwarz, T, Saunders, J. CT acquisitation principle. In: Schwarz, T, Saunders, J, eds. Veterinary computed tomography. 1st ed. Oxford: Wiley-Blackwell; 2011, p.9-27.

Seel, EH, Davies, EM. A biomechanical comparison of kyphoplasty using a balloon bone tamp versus an expandable polymer bone tamp in a deer spine model. J Bone Joint Surg Br. 2007;89:253-7.

Seiler, G, Kinns, J., Dennison, S., Saunders, J., Schwarz, T. Vertebral column and spinal cord. In: Schwarz, T, Saunders, J, eds. Veterinary computed tomography. Oxford: Wiley-Blackwell; 2011, p.209-28.

Sen, A, Santra, A, Karim, S. Carcass yield, composition and meat quality attributes of sheep and goat under semiarid conditions. Meat Sci. 2004;66:757-63.

Senel, A, Tanik, A, Akan, H. Quantitative assessment of the normal adult spinal canal at the fourth lumbar vertebra by computed tomography. Neuroradiology. 1994;36:54-5.

Sharp, NJ, Cofone, M, Robertson, ID, DeCarlo, A, Smith, GK, Thrall, DE. Computed tomography in the evaluation of caudal cervical spondylomyelopathy of the Doberman Pinscher. Vet Radiol Ultrasound. 1995;36:100-8.

Sheng, S-R, Wang, X-Y, Xu, H-Z, Zhu, G-Q, Zhou, Y-F. Anatomy of large animal spines and its comparison to the human spine: a systematic review. Eur Spine J. 2010;19:46-56.

Sherman, J, Nassaux, P, Citrin, C. Measurements of the normal cervical spinal cord on MR imaging. Am J Neuroradiol. 1990;11:369-72.

Sicard, JA, Forestier, J. Méthode radiologique d'exploration de la cavité épidurale par le lipiodol. Revista de Neurología. 1921;28:1264–66.

Smit, TH. The use of a quadruped as an in vivo model for the study of the spine-biomechanical considerations. Eur Spine J. 2002;11:137-44.

Soubeyrand, M, Laemmel, E, Dubory, A, Vicaut, E, Duranteau, J. Rat model of spinal cord injury preserving dura mater integrity and allowing measurements of cerebrospinal fluid pressure and spinal cord blood flow. Eur Spine J. 2013;1-10.

Söyüncü, Y, Yldrm, FB, Sekban, H, Özdemir, H, Akyldz, F, Sindel, M. Anatomic evaluation and relationship between the lumbar pedicle and adjacent neural structures: an anatomic study. J Spinal Disord Tech. 2005;18:243-6.

Tatarek, NE. Variation in the human cervical neural canal. Spine J. 2005;5:623-31.

Tierney, RT, Maldjian, C, Mattacola, CG, Straub, SJ, Sitler, MR. Cervical spine stenosis measures in normal subjects. J Athl Train. 2002;37:190-3.

Tins, B. Technical aspects of CT imaging of the spine. Insights imaging. 2010;1:349-59.

Tominaga, T, Dickman, CA, Sonntag, V, Coons, S. Comparative anatomy of the baboon and the human cervical spine. Spine. 1995;20:131-7.

Turan Suslu, H, Tatarli, N, Hicdonmez, T, Borekci, A. A laboratory training model using fresh sheep spines for pedicular screw fixation. Br J Neurosurg. 2012;26:252-4.

Turner, AS. Animal models of osteoporosis—necessity and limitations. Eur Cell Mater. 2001;22:66-81.

Turner, AS. Experiences with sheep as an animal model for shoulder surgery: strengths and shortcomings. J Shoulder Elbow Surg. 2007;16:S158-63.

Vaccaro, AR, Nachwalter, RS, Klein, GR, Sewards, JM, Albert, TJ, Garfin, SR. The significance of thoracolumbar spinal canal size in spinal cord injury patients. Spine. 2001;26:371-6.

Wall, EJ, Bylski-Austrow, DI, Shelton, FS, Crawford, AH, Kolata, RJ, Baum, DS. Endoscopic discectomy increases thoracic spine flexibility as effectively as open discectomy. A mechanical study in a porcine model. Spine. 1998;23:9-15.

Way, TW, Chan, H-P, Goodsitt, MM, Sahiner, B, Hadjiiski, LM, Zhou, C, Chughtai, A. Effect of CT scanning parameters on volumetric measurements of pulmonary nodules by 3D active contour segmentation: a phantom study. Phys Med Biol. 2008;53:1295-312.

Wilke, HJ, Wenger, K, Claes, L. Testing criteria for spinal implants: recommendations for the standardization of in vitro stability testing of spinal implants. Eur Spine J. 1998;7:148-54.

Wilke, HJ, Kettler, A, Wenger, KH, Claes, LE. Anatomy of the sheep spine and its comparison to the human spine. Anat Rec. 1997a;247:542-55.

Wilke, HJ, Kettler, A, Claes, LE. Are sheep spines a valid biomechanical model for human spines? Spine. 1997b;22:2365-74.

Wolf, A, Shoham, M, Michael, S, Moshe, R. Morphometric Study of the Human Lumbar Spine for Operation–Workspace Specifications. Spine. 2001;26:2472-7.

Worth, HM. The use of lipiodol in the localisation of spinal tumours. Br J Rheumatol. 1938;11:211–26.

Yoganandan, N, Kumaresan, S, Voo, L, Pintar, FA. Finite element applications in human cervical spine modeling. Spine. 1996;21:1824-34.

Yu, Y, Du Boulay, G, Stevens, J, Kendall, B. Computed tomography in cervical spondylotic myelopathy and radiculopathy: visualisation of structures, myelographic comparison, cord measurements and clinical utility. Neuroradiology. 1986;28:221-36.

Zarrinkalam, M, Beard, H, Schultz, CG, Moore, RJ. Validation of the sheep as a large animal model for the study of vertebral osteoporosis. Eur Spine J. 2009;18:244-53.

Zhou, S, McCarthy, I, McGregor, A, Coombs, R, Hughes, S. Geometrical dimensions of the lower lumbar vertebrae–analysis of data from digitised CT images. Eur Spine J. 2000;9:242-8.

Zindrick, MR, Wiltse, LL, Doornik, A, Widell, EH, Knight, GW, Patwardhan, AG, Thomas, JC, Rothman, SL, Fields, B. Analysis of the morphometric characteristics of the thoracic and lumbar pedicles. Spine. 1987;12:160-6.

8 Acknowledgement

I have been very fortunate with my supervisors **Prof. Walter Brehm** and **Dr. Kerstin Gerlach**, for supporting me during these past three and half years.

My sincere thanks also go to **Dr. Eberhard Ludewig, Dr. Dagmar Berner** and **Dr. Jean-Claude Ionita** for helping me through the practical parts and their comments and advices.

I would like to thank the Institute of Veterinary Physiology particularly Ms. Franziska Benesch for providing the animal for the experiments.

I wish to thank **Gunhild Berndt**, **Andreas Malter** and **Miguel Espina**, for encouraging and supporting me with my work. I also thank all the present **members of the Large Animal Clinic for Surgery** for supporting me during the past three years.

It would not have been possible to write this doctoral thesis without the help and support of the kind people around me, to only some of whom it is possible to give particular mention here.

Last but not the least, I would like to thank my family: my parents **Abd El-Moniem** and **Samira**, for giving birth to me at the first place and supporting me spiritually throughout my life; My darling wife **Shahlaa** and our beloved daughter **Hannen** for their encouragements and understanding.

For any errors or inadequacies that may remain in this work, of course, the onus is entirely my own.

Mahmoud Mageed

2014